4OR (2020) 18:249–292
https://doi.org/10.1007/s10288-020-00455-w

INVITED SURVEY

Mathematical programming formulations for the alternating current optimal power flow problem

Dan Bienstock[1] · Mauro Escobar[2] · Claudio Gentile[3] · Leo Liberti[2]

Received: 1 July 2020 / Revised: 9 August 2020 / Published online: 15 September 2020

Abstract

Power flow refers to the injection of power on the lines of an electrical grid, so that all the injections at the nodes form a consistent flow within the network. Optimality, in this setting, is usually intended as the minimization of the cost of generating power. Current can either be direct or alternating: while the former yields approximate linear programming formulations, the latter yields formulations of a much more interesting sort: namely, nonconvex nonlinear programs in complex numbers. In this technical survey, we derive formulation variants and relaxations of the alternating current optimal power flow problem.

Keywords ACOPF · Smart grid · Complex numbers

Mathematics Subject Classification 90C90 · 90C26

CG was partly supported by the Italian Ministry of Education under the PRIN 2015B5F27W project "Nonlinear and conditional aspects of complex networks". DB and LL benefitted from an exchange between Ecole Polytechnique and Columbia University financed by Columbia Alliance. CG and LL have received funding from the European Union's Horizon 2020 research and innovation programme under the Marie Sklodowska-Curie Grant Agreement No. 764759 "MINOA". LL was partially supported by CNR STM Program Prot. AMMCNT–CNR No. 16442 dated 05/03/2018 and by INDAM Visiting Professors program 2018 prot. U-UFMBAZ-2017-001577 dated 22/12/2017.

✉ Leo Liberti
liberti@lix.polytechnique.fr

Dan Bienstock
dano@columbia.edu

Mauro Escobar
escobar@lix.polytechnique.fr

Claudio Gentile
gentile@iasi.cnr.it

1 IEOR, Columbia University, New York, USA

2 LIX CNRS, Ecole Polytechnique, Institut Polytechnique de Paris, Palaiseau, France

3 IASI, CNR, Rome, Italy

Contents

1 Introduction

This paper is about Mathematical Programming (MP) formulations for the Alternating Current Optimal Power Flow (ACOPF) problem. The ACOPF is an optimization problem aiming at generating and transporting electrical power at minimum cost.

The basic entity in electricity is the *charge*: by analogy, charge is to the electromagnetic force what mass is to gravity. Charge is transported in electrical cables: it thus makes sense to measure how much charge is passing through the cable at a given point in a second. Such a measure is called *current*: charge per unit surface per unit time. For any portion of space one may define an *electric field*, consisting of a vector at each point representing the (directed) force acting on a unit charge (think of the analogy with a gravitational field, representing force on a unit mass). The *voltage* is

the potential energy of a unit charge in the electric field. Finally, the *power* is measured as voltage multiplied by current.

The transportation of power from generating plants (or *generators*) to users (or *loads*) occurs by means of a network, called *power grid*, the nodes of which are called *buses* and the links *lines* (or, sometimes, *branches*). Buses may be hubs, relays, buildings or entire corporations; lines consist of electrical cables linking two buses. Generators are assigned to buses, so that a bus may be a load, but may also, at the same time, host a varying number of generators.

Electrical networks may transport Direct Current (DC) or Alternating Current (AC). Small electronic devices, such as radios, televisions, computers, are usually driven by DC. The transportation of power on any geographical area is typically based on AC. This occurs naturally when transforming kinetic energy, e.g. from a waterfall, to a rotating wheel with some attached magnets. While the magnetic wheel rotates, the alternating magnetic field induces an alternating electrical field (in accordance with Maxwell's equations) which in turn induces an alternating current in an appropriately placed cable. The frequency of the rotation goes from 50 to 60 Hz depending on country.

While charge (in the form of electrons) actually moves along the cable in DC, in AC the charge moves very little. It "oscillates" in the cable, according to the alternating nature of the electrical field it is subjected to, and generates an electromagnetic wave which propagates along the material of the cables at some significant fraction of the speed of light (the electrons themselves move much more slowly). This wave induces a power flow along the lines. The power is induced by the current and the voltage difference between the buses incident to the line. For a line ℓ incident to buses b, a, power is "injected" in ℓ at b (in one direction) and at a (in the other direction, with directions changing according to the field oscillations).

Electricity production stakeholders have an interest in generating sufficient power to satisfy demand. In doing so, they also have to make sure that the power can be transported from the generating bus, over the lines of the electrical networks, to the load bus. The ACOPF is supposed to achieve this purpose.

The rest of this paper is organized as follows. We explain how a time-dependent problem can be modelled using formulations that do not depend on time in Sect. 2. We discuss the basic modelling of the ACOPF using MP in Sect. 3. We propose some formulations in complex numbers in Sect. 4, and explain how to obtain formulations in real numbers in Sect. 5. We provide a literature review in Sect. 6, which focuses mostly on contributions of the theory of ACOPF relaxations (Sect. 6.6). Sect. 7 concludes the paper.

2 Dealing with the time dependency

From Sect. 1, it should be clear that optimized generation of AC power in power grids is in fact a dynamic problem, also known as a *mathematical control* problem. Time plays a factor insofar as energy is expressed as a wave having frequency ω. Current, voltage and power values oscillate with the same frequency ω according to the corresponding relationships. We denote current on the line ℓ adjacent to b, a by

I_{ba}, voltage at bus b by V_b and power injected in ℓ at b by S_{ba}. As functions of time t, we have the following relationships (Bienstock 2016, p. 3):

$$\begin{aligned} V_b(t) &= V_b^{\max} \cos(\omega t + \theta_b) \\ I_{ba}(t) &= I_{ba}^{\max} \cos(\omega t + \phi_{ba}) \\ S_{ba}(t) &= V_b(t) I_{ba}(t), \end{aligned} \tag{1}$$

where $V_b^{\max}$, $I_{ba}^{\max}$ are amplitudes and θ_b, ϕ_{ba} are phases of voltage at a bus b and of current at an incident line leading to bus a.

By Eq. (1), using basic trigonometric relations, we obtain:

$$\begin{aligned} S_{ba}(t) &= V_b^{\max} I_{ba}^{\max} \cos(\omega t + \theta_b) \cos(\omega t + \phi_{ba}) = \\ &= \frac{1}{2} V_b^{\max} I_{ba}^{\max} (\cos(\theta_b - \phi_{ba}) + \cos(2\omega t + \theta_b + \phi_{ba})). \end{aligned}$$

Formulating a time-dependent ACOPF is certainly possible using these time-dependent quantities, but it would be infeasible to find a solution for real-life cases using current computational technology. Instead, we consider steady state average values over a period $2\pi/\omega$, which we simply indicate with I, V, S without the dependence on t. For the usual bus b and its incident line linking it to bus a, we then obtain [Bienstock 2016, Eq. (1.3)]:

$$S_{ba} = \frac{1}{2} V_b^{\max} I_{ba}^{\max} \cos(\theta_b - \phi_{ba}), \tag{2}$$

to which there correspond averages for V, I too.

Restricting the analysis of a whole function $S(t)$ to its average S causes a loss of information which is deemed excessive. An ACOPF only defined on the averages I, V, S apparently fails to capture many phenomena that are important to robust power grid design. An acceptable compromise is reached by considering I, V, S as complex instead of real quantities. The averages computed above are then considered their real parts I^{r}, V^{r}, S^{r}; and their imaginary parts I^{c}, V^{c}, S^{c} provide a further piece of (static) information about the dynamics of $I(t)$, $V(t)$, $S(t)$ as functions of time.

We therefore write cartesian and polar representations of voltage, current and power as complex quantities:[1]

$$\begin{aligned} V_b &= V_b^{\mathrm{r}} + i\, V_b^{\mathrm{c}} = \frac{V_b^{\max}}{\sqrt{2}} e^{i\theta_b} \\ I_{ba} &= I_{ba}^{\mathrm{r}} + i\, I_{ba}^{\mathrm{c}} = \frac{I_{ba}^{\max}}{\sqrt{2}} e^{i\phi_{ba}} \\ S_{ba} &= S_{ba}^{\mathrm{r}} + i\, S_{ba}^{\mathrm{c}} = |S_{ba}| e^{i\psi_{ba}}, \end{aligned}$$

[1] We remark that most of the power grid literature uses i to indicate current, and therefore resorts to j to indicate $\sqrt{-1}$. We chose to keep notation in line with mathematics and the rest of the physical sciences, namely we use $i = \sqrt{-1}$, and employ I to denote current.

where ψ_{ba} is the phase for power. We now reformulate Eq. (2) as

$$S^{\mathsf{r}}_{ba} = |V_b||I_{ba}|\cos(\theta_b - \phi_{ba}) = (V_b\, I_{ba}{}^*)^{\mathsf{r}},$$

where $x^* = x^{\mathsf{r}} - i\,x^{\mathsf{c}}$ is the *complex conjugate* of x, and $|x| = \sqrt{x\,x^*} = \sqrt{(x^{\mathsf{r}})^2 + (x^{\mathsf{c}})^2}$ is the *modulus*, of any $x \in \mathbb{C}$.

Thus, it makes sense to define an "imaginary power"

$$S^{\mathsf{c}}_{ba} = (V_b\, I_{ba}{}^*)^{\mathsf{c}},$$

yielding a complex power $S_{ba} = S^{\mathsf{r}}_{ba} + i\,S^{\mathsf{c}}_{ba}$. In the power grid literature, real power is known as *active power*, while imaginary power is known as *reactive power*.

2.1 Change of coordinates

In the rest of this paper, we will construct various ACOPF formulations based on I_b, V_{ba}, $S_{ba} \in \mathbb{C}$ for any bus b and any line ℓ incident to b, a. In particular, we will use both the cartesian and the polar representations of complex numbers. In this section we recall the nonlinear transformation relations between these representations.

Consider $x = x^{\mathsf{r}} + i\,x^{\mathsf{c}} \in \mathbb{C}$ expressed in cartesian coordinates. The polar representation of x is $\alpha e^{i\,\vartheta} = \alpha\cos\vartheta + i\alpha\sin\vartheta$, where α is the magnitude and ϑ is known as the *angle* or *phase* of the complex number (which is itself also called *phasor*).

The change of coordinates from cartesian to polar representations (and vice versa) is a nonlinear relationship between x^{r}, x^{c} and α, ϑ, as follows:

$$\begin{array}{ll} x^{\mathsf{r}} = \alpha\cos\vartheta & \alpha = \sqrt{(x^{\mathsf{r}})^2 + (x^{\mathsf{c}})^2} \\ x^{\mathsf{c}} = \alpha\sin\vartheta & \vartheta = \arccos(x^{\mathsf{r}}/\alpha) = \arcsin(x^{\mathsf{c}}/\alpha), \end{array}$$

where we take the positive sign of the square root for α. We further remark that the following identities are often used in complex derivations:

$$\forall x \in \mathbb{C} \quad 2x^{\mathsf{r}} = x + x^* \tag{3}$$

$$\forall x \in \mathbb{C} \quad -2x^{\mathsf{c}} = i(x - x^*). \tag{4}$$

3 Modelling the ACOPF

MP formulations for the ACOPF are unlike every other formulation we have ever seen, in that they require an unusual amount of effort to understand, and an inordinate amount of debugging to implement. Many OR researchers and practitioners do not use complex numbers in their normal line of work, so this is part of the difficulty. Another part is the way the input data is presented and stored, which may be natural to electrical engineers, but certainly did not seem natural to us. In this section we will do our best to explain the modelling difficulties away, and to warn the reader against the implementation pitfalls we found.

We remark that electrical engineers themselves do not all agree on the way to approximate dynamic behaviour by static quantities, nor on the notation used. We refer to the well-known, high quality, open-source and *de facto* standard-establishing MATLAB software MATPOWER (Zimmermann et al. 2010), as well as to its user manual (Zimmermann and Murillo-Sánchez 2018), as a reference to what we mean by the expression of an ACOPF MP formulation, and its related notation, by electrical engineers. Other examples of typical notation and formulation style in use in the AC power community are given in Cain et al. (2012).

3.1 The power grid as a graph

The power grid is a network of buses interconnected by lines. The standard abstract entity used to model networks is a graph. In this case, however, there are a few unusual modelling issues.

1. The first modelling issue is that a line, which models a cable, is not always an undirected edge: whenever the line ℓ between buses b, a has a transformer close to the b end, the current and injected power on ℓ at b is different from that at a (in DC, by contrast, the current injected on ℓ at b is equal to the negative of the current injected at a). This, in general, points us towards a directed graph, or *digraph*, where each line is modelled as a pair of anti-parallel arcs $\{(b, a), (a, b)\}$.
2. We remark that if ℓ hosts a transformer, (b, a) and (a, b) have different current and injected power values; moreover, they have voltage differences with same magnitude and opposite signs. This raises a second issue. The relationship of current and voltage for the two antiparallel arcs is expressed by a vectorial equation in two components (one for (b, a) and one for (a, b)), where a 2-component current vector I_{ba} is given as a 2×2 non-symmetric admittance matrix $\mathbf{Y}_{ba}$ multiplying a 2-component voltage vector $\mathbf{V}_{ba}$ (voltage at b and voltage at a):

$$\mathbf{I}_{ba} = \mathbf{Y}_{ba}\mathbf{V}_{ba}. \tag{5}$$

   This modelling technique also applies to injected power because of the equation $S_{ba} = V_b\, I_{ba}{}^*$. We shall see that one of the terms in the power flow equations (see Sect. 3.3) is the sum $\sum_{(b,a)} S_{ba}$ of injected powers S_{ba}, at a bus b, over all the lines incident to b. For obvious topological reasons, this sum never involves pairs of antiparallel arcs $(b, a), (a, b)$. Instead, it may involve arcs (b, a_1) (for some bus a_1 adjacent to b) where the transformer is at b, and arcs (b, a_2) where the transformer is at a_2 (for some other bus a_2 adjacent to b). This means that we must pick the first component of the 2-vector current-voltage equation Eq. (5) for (b, a_1) and the second component of Eq. (5) for (a_2, b), which requires considerable care with handling indices. This issue is discussed in more depth in Sect. 4.2.
3. A third issue is given by the fact that sometimes parallel cables transport power between two buses in the case when one cable would be insufficient for the power demand. This means there may be parallel lines $\ell_1, \ldots, \ell_p$ between two buses b, a, and that each must be modelled as a pair of anti-parallel arcs. This is

an unusual setting insofar as MP formulations on graphs go, which contributes to the modelling difficulty associated with the ACOPF. We remark that each arc going from b to a may have different values of power and current, but the same voltage difference associated to b and a. Since the equations regulating power and current are nonlinear, it is not possible to model sheaves of parallel arcs by a single arc which aggregates the values of each arc in the sheaf.

3.2 The π-model of a line

We introduce some of the parameter and decision variable symbols in the ACOPF by means of the so-called "π-model" of a line (Fig. 1).

The graphical representation of a line consists of two horizontal parallel segments. The above segment represents the line, going from bus b (on the left) to bus a (on the right). The segment below corresponds to the ground: if we were using DC, electrons flowing from b to a would need to come back from a back to b using the ground.

The pair of vertical parallel coils on the left represents a transformer installed at b: the parameter $N_{ba} \in \mathbb{C}$, the "ratio" of the AC transformation, is sometimes indicated by $N_{ba} : 1$, but N_{ba} is *not* necessarily an integer; in general, it is a complex number. It is usually expressed in its polar representation $N_{ba} = \tau_{ba} e^{i\nu_{ba}}$, where τ_{ba} is the magnitude and ν_{ba} the angle.

Next, going from left to right, we find the voltage V_b, expressed as a voltage difference between potential energy at b and at the ground. Above the top segment we find a sequence of symbols: the injected power $\overrightarrow{S}_{ba}$ at b, the current $\overrightarrow{I}_{ba}$ at b, then the *series impedance* $y_{ba} = r_{ba} + ix_{ba}$ of the line ℓ between b and a, and then the corresponding injections $\overleftarrow{S}_{ba}$, $\overleftarrow{I}_{ba}$ at a. Below, we find the complex terms $i\mathfrak{b}_{ba}/2$, where $\mathfrak{b}_{ba}$ is the *line charging susceptance* (an interaction of the line with the ground).

The 2×2 matrix $\mathbf{Y}_{ba}$ referred to above is defined follows.

$$\mathbf{Y}_{ba} = \begin{pmatrix} Y_{ba}^{\mathsf{ff}} & Y_{ba}^{\mathsf{ft}} \\ Y_{ba}^{\mathsf{tf}} & Y_{ba}^{\mathsf{tt}} \end{pmatrix} = \begin{pmatrix} \left(\frac{1}{r_{ba}+ix_{ba}} + i\,\frac{\mathfrak{b}_{ba}}{2}\right)/\tau_{ba}^2 & -\frac{1}{(r_{ba}+ix_{ba})\tau e^{-i\nu_{ba}}} \\ -\frac{1}{(r_{ba}+ix_{ba})\tau_{ba} e^{i\nu_{ba}}} & \frac{1}{r_{ba}+ix_{ba}} + i\,\frac{\mathfrak{b}_{ba}}{2} \end{pmatrix}, \tag{6}$$

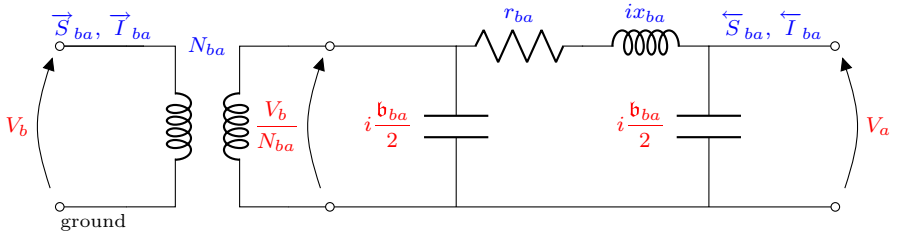

Fig. 1 The π-model of a line

where the suffixes ff, ft, tf, tt stand for "from-from", "from-to", "to-from", and "to-to", which are a reminder for the direction referring to b, a. Such suffixes help addressing the second issue mentioned in Sect. 3.1, as we shall also see in Sect. 4.2 below.

We note that $\mathbf{Y}_{ba}$ is sometimes also expressed in function of $z_{ba} = \frac{1}{y_{ba}}$ as follows:

$$\mathbf{Y}_{ba} = \begin{pmatrix} (z_{ba} + i\frac{\mathfrak{b}_{ba}}{2})/\tau_{ba}^2 & -z_{ba}/(\tau e^{-i\nu_{ba}}) \\ -z_{ba}/(\tau_{ba} e^{i\nu_{ba}}) & z_{ba} + i\frac{\mathfrak{b}_{ba}}{2} \end{pmatrix}.$$

From Eqs. (5) and (6), we see the reason why the current on a line ℓ between b and a and hosting a transformer at b is different depending on whether it flows from b or a. We have:

$$\overrightarrow{I}_{ba} = Y_{ba}^{\mathsf{ff}} V_b + Y_{ba}^{\mathsf{ft}} V_a \tag{7}$$

$$\overleftarrow{I}_{ba} = Y_{ba}^{\mathsf{tf}} V_b + Y_{ba}^{\mathsf{tt}} V_a, \tag{8}$$

and it is clear from Eq. (6) that Eq. (7) and Eq. (8) are different. On the other hand, Eq. (6) also shows us that, if no transformer is installed at the line, then we have $N_{ab} = 1$, which makes $\mathbf{Y}_{ba}$ symmetric. If, moreover, the line charging susceptance $\mathfrak{b}_{ba}$ is zero, we have $\overrightarrow{I}_{ba} = -\overleftarrow{I}_{ba}$: namely, the alternating current on the line behaves like direct current.

In this section we have denoted directed power and currents by means of arrows over the corresponding symbols $\overrightarrow{S}_{ba}$, $\overleftarrow{S}_{ba}$, $\overrightarrow{I}_{ba}$, $\overleftarrow{I}_{ba}$ for clarity w.r.t. a given line ℓ between b, a. Since our formulations below are based on a digraph representation of the network, we shall use the corresponding (directed) arc expressions $S_{ba}, S_{ab}, I_{ba}, I_{ab}$. Moreover, if there are p_{ba} parallel lines between b and a, we use symbols $S_{bah}, S_{abh}, I_{bah}, I_{abh}$ for $h \leq p_{ba}$; the symbols $r, x, \tau, \nu, \mathfrak{b}$ are all indexed by b, a, h (for $h \leq p_{ba}$); and, consequently, this also holds for the symbols $y, z, Y^{\mathsf{ff}}, Y^{\mathsf{ft}}, Y^{\mathsf{tf}}, Y^{\mathsf{tt}}, \mathbf{Y}$.

3.3 Informal description of ACOPF formulations

MP formulations for the ACOPF consist of:

- an objective function, which usually minimizes the cost of the generated power;
- a set of bound constraints:
  - on the voltage magnitude;
  - on the difference of voltage angles between adjacent buses;
  - on the maximum power magnitude injected on a line (such bounds may be alternatively be imposed on the maximum current);
  - on the generated power;
- a set of explicit constraints:
  - on the power balance at each bus (also called "power flow equations");
  - on the definition of power in function of voltage and current;

– on the definition of current w.r.t. voltage [an AC generalization of Ohm's equation, see Eq. (5)].

There may be other technical constraints, depending on the network at hand, and the application requiring the solution of the ACOPF. The MATPOWER software (Zimmerman et al. 2010), for example, provides a "reference" status for each bus. A "reference bus" has the voltage angle (a.k.a. phase) set to zero.

4 Complex formulations

In this section we shall discuss some ACOPF formulations where the decision variables are in $\mathbb{C}$.

4.1 The (*S*, *I*, *V*)-formulation

We first present what we consider to be the most basic ACOPF formulation, in terms of power S, current I and voltage V.

4.1.1 Sets, parameters and decision variables

Index sets and parameters represent the input of a MP formulation. The decision variables will encode the solution after an appropriate algorithm has solved the formulation.

We consider a multi-digraph $G = (B, L)$ where B is the set of buses, and L is the set of arcs representing the lines. We assume $|B| = n$ and $|L| = m$. L is partitioned in two sets L_0, L_1 with $|L_0| = |L_1|$, which makes $|L|$ even: this is consistent with the fact that every line is represented by two anti-parallel arcs. For the hth line ℓ_h between b, a, for $h \leq p_{ba}$, represented by a set of anti-parallel arcs $\{(b, a, h), (a, b, h)\}$, exactly one between the anti-parallel arcs, say (b, a, h), belongs to L_0, and the other, (a, b, h), belongs to L_1. In particular, every line ℓ_h with a transformer at b is oriented so that $(b, a, h) \in L_0$ and $(a, b, h) \in L_1$.

We also consider a set $\mathscr{G}$ of generators, partitioned into (possibly empty) subsets $\mathscr{G}_b$ for every $b \in B$. The generators in $\mathscr{G}_b$ are those that are assigned to bus b.

We consider the following parameters.

1. The objective function is a real-valued polynomial of degree d of the power generated at $g \in \mathscr{G}$. The coefficients $c_{g0}, \ldots, c_{g,d-1}$ are given for all $g \in \mathscr{G}$.
2. Voltage.
   – At each bus $b \in B$ the voltage magnitude $|V_b|$ is constrained to lie in a given real range $[\underline{V}_b, \overline{V}_b]$.
   – At each arc $(b, a, h) \in L_0$, the voltage phase difference $\theta_b - \theta_a$ between b and a is constrained to lie in a given real range $[\underline{\eta}_{bah}, \overline{\eta}_{bah}]$. Since the voltage phase difference w.r.t. (a, b, h) is simply the same for (b, a, h) in absolute value, we do not need to impose these constraints for arcs in L_1. In fact, it suffices to impose the most restrictive bounds for each unordered pair $\{b, a\}$.

– A chosen bus index $r \in B$ is designated as "reference", which entails having voltage phase $\theta_r = 0$; by setting $V_r^{\mathsf{r}} + iV_r^{\mathsf{c}} = |V_r|e^{i\theta_r}$, we see that $\theta_r = 0$ implies $V_r^{\mathsf{c}} = 0$ and $V_r^{\mathsf{r}} = |V_r|$.

3. Power.
   – The power demand at bus $b \in B$ is denoted $\tilde{S}_b \in \mathbb{C}$; there can be buses with negative demand (i.e. more generation than demand).
   – At each arc $(b, a, h) \in L$ the magnitude $|S_{bah}|$ of the power injected on the line is constrained to be bounded above by a real scalar $\bar{S}_{bah} \geq 0$. This bound does not depend on the injection direction, so $\bar{S}_{bah} = \bar{S}_{abh}$.
   – At each generator $g \in \mathcal{G}_b$ installed at bus $b \in B$ the power at g is constrained to be within complex ranges $[\underline{\mathscr{S}}_g, \overline{\mathscr{S}}_g]$ (meaning that the real part is in $[\underline{\mathscr{S}}_g^{\mathsf{r}}, \overline{\mathscr{S}}_g^{\mathsf{r}}]$ and the imaginary part is in $[\underline{\mathscr{S}}_g^{\mathsf{c}}, \overline{\mathscr{S}}_g^{\mathsf{c}}]$).

4. Current.
   – For every arc $(b, a, h) \in L_0$ we are given the matrix $\mathbf{Y}_{bah} \in \mathbb{C}^{2\times 2}$. The first row of each $\mathbf{Y}_{bah}$ defines current in function of voltage for the direction from b to a, while the second row handles the opposite direction, see Eq. (7) and (8). So we do not need to define these matrices over arcs in L_1.
   – At each arc $(b, a, h) \in L$ the current magnitude $|I_{bah}|$ may be constrained to be bounded above by a real scalar $\bar{I}_{bah} \geq 0$, such that $\bar{I}_{bah} = \bar{I}_{abh}$. This bound is usually enforced as an alternative to the injected power bound $\bar{S}$, see Sect. 4.3.

5. The *shunt admittance* at bus $b \in B$, related to an interaction with the ground, is $A_b \in \mathbb{C}$.

We consider the following decision variables.

(a) The complex voltage at each bus $b \in B$ is denoted $V_b \in \mathbb{C}$.
(b) The complex current at each arc $(b, a, h) \in L$ is denoted $I_{bah} \in \mathbb{C}$. For each pair of antiparallel arcs $(b, a, h) \in L_0$ and $(a, b, h) \in L_1$, we define the vector $\mathbf{I}_{bah} = (I_{bah}, I_{abh})^\top \in \mathbb{C}^2$.
(c) The complex power at each arc $(b, a, h) \in L$ (injected at b) is denoted $S_{bah} \in \mathbb{C}$. For each pair of antiparallel arcs $(b, a, h) \in L_0$, $(a, b, h) \in L_1$, we define the vector $\mathbf{S}_{bah} = (S_{bah}, S_{abh})^\top \in \mathbb{C}^2$.
(d) For a generator $g \in \mathcal{G}_b$ installed at bus $b \in B$, $\mathscr{S}_g$ is the complex power generated by g.

4.1.2 Objective and constraints

The most elementary objective function employed in MATPOWER (Zimmermann et al. 2010) is a polynomial function of degree d of (real) generated power:

$$\min \sum_{g\in\mathcal{G}} \sum_{j=0}^{d} c_{g,d-j} (\mathscr{S}_g^{\mathsf{r}})^{d-j}. \tag{9}$$

We also consider two simpler objective functions. One of them, with $d = 2$, involves a Hermitian quadratic form (namely, with the complex square matrix Q being equal to its conjugate transpose):

$$\min(\mathscr{S}^{\mathsf{H}} Q \mathscr{S} + c_1 \mathscr{S}^{\mathsf{r}} + c_0), \tag{10}$$

where $\mathscr{S} = (\mathscr{S}_g \mid g \in \mathscr{G})$, $c_1 = (c_{g1} \mid g \in \mathscr{G})$, $c_0 = (c_{g0} \mid g \in \mathscr{G})$. This makes this formulation a complex Quadratically Constrained Quadratic Program (QCQP) in function of power. Another one, with $d = 1$,

$$\min \sum_{g \in \mathscr{G}} (c_{g1} \mathscr{S}_g^{\mathsf{r}} + c_{g0}), \tag{11}$$

yields a Quadratically Constrained Program (QCP) which is linear in generated power. Eq. (11) is going to be used in the voltage-only formulation of Sect. 4.3 so as to obtain a QCQP in voltage.

We consider the following bound constraints.

– Lower/upper bounds on generated power are imposed at every generator:

$$\forall b \in B, g \in \mathscr{G}_b \quad \underline{\mathscr{S}}_g \leq \mathscr{S}_g \leq \overline{\mathscr{S}}_g. \tag{12}$$

– The upper bounds on power magnitudes (squared, since polynomial formulations are preferred) are imposed at every arc:

$$\forall (b, a, h) \in L \quad |S_{bah}|^2 \leq \bar{S}_{bah}^2, \tag{13}$$

where we recall that $\bar{S}_{bah} = \bar{S}_{abh}$.

– The bounds $[\underline{\eta}_{bah}, \overline{\eta}_{bah}]$ on the phase difference cannot be imposed directly, as the voltage phase does not appear as a decision variable. From the polar representation $x = |x| e^{i\vartheta}$ one could argue $\vartheta = -i \ln(x/|x|)$, but this would prevent the formulation from being quadratic in its variables. Instead, we proceed as follows. We select an appropriate monotonically increasing function and write the original constraints:

$$\forall (b, a, h) \in L_0 \quad \underline{\eta}_{bah} \leq \theta_b - \theta_a \leq \overline{\eta}_{bah}$$

as

$$\forall (b, a, h) \in L_0 \quad \tan(\underline{\eta}_{bah}) \leq \tan(\theta_b - \theta_a) \leq \tan(\overline{\eta}_{bah}),$$

where we assume that $-\pi/4 < \underline{\eta}_{bah} \leq \overline{\eta}_{bah} < \pi/4$. This assumption is justified in the following sense: either these constraints are inactive, in which case they need not be enforced, or else, in practice, $\overline{\eta}_{bah} - \underline{\eta}_{bah}$ is usually smaller than $\pi/2$. Next, we note that

$$\tan(\theta_b - \theta_a) = \frac{\sin(\theta_b - \theta_a)}{\cos(\theta_b - \theta_a)} = \frac{|V_b|\,|V_a| \sin(\theta_b - \theta_a)}{|V_b|\,|V_a| \cos(\theta_b - \theta_a)}$$

$$= \frac{|V_b| \sin\theta_b |V_a| \cos\theta_a - |V_b| \cos\theta_b |V_a| \sin\theta_a}{|V_b| \cos\theta_b |V_a| \cos\theta_a + |V_b| \sin\theta_b |V_a| \sin\theta_a}$$
$$= \frac{V_b^{\mathsf{c}} V_a^{\mathsf{r}} - V_b^{\mathsf{r}} V_a^{\mathsf{c}}}{V_b^{\mathsf{r}} V_a^{\mathsf{r}} + V_b^{\mathsf{c}} V_a^{\mathsf{c}}} = \frac{(V_b\, V_a^*)^{\mathsf{c}}}{(V_b\, V_a^*)^{\mathsf{r}}},$$

whence the desired constraints can be written as:

$$\begin{aligned} \forall (b,a,h) \in L_0 \;\; & \tan(\underline{\eta}_{bah}) \le \tfrac{(V_b\, V_a^*)^{\mathsf{c}}}{(V_b\, V_a^*)^{\mathsf{r}}} \le \tan(\overline{\eta}_{bah}) \\ \Rightarrow \;\; & \tan(\underline{\eta}_{bah})(V_b\, V_a^*)^{\mathsf{r}} \le (V_b\, V_a^*)^{\mathsf{c}} \le \tan(\overline{\eta}_{bah})(V_b\, V_a^*)^{\mathsf{r}} \end{aligned} \tag{14}$$

provided the additional constraints:

$$\forall (b,a,1) \in L_0 \quad (V_b\, V_a^*)^{\mathsf{r}} \ge 0 \tag{15}$$

hold. We remark that Eqs. (14) and (15) are both quadratic in voltage, and recall that we assume $[\underline{\eta}_{bah}, \overline{\eta}_{bah}] \subset [-\pi/4, \pi/4]$. Note that Eq. (15) can be strengthened by requiring

$$\forall (b,a,1) \in L_0 \quad \overline{V}_b \overline{V}_a \max\{0, \cos(\underline{\eta}_{bah}), \cos(\overline{\eta}_{bah})\} \le (V_b\, V_a^*)^{\mathsf{r}} \le \overline{V}_b \overline{V}_a.$$

– Lower/upper bounds on the voltage magnitude are imposed at each bus:

$$\forall b \in B \quad \underline{V}_b^2 \le |V_b|^2 \le \overline{V}_b^2. \tag{16}$$

– At the reference bus $r \in B$, we have $V_r^{\mathsf{c}} = 0$; as mentioned above, this makes $V_r^{\mathsf{r}} = |V_r|$, implying

$$V_r^{\mathsf{c}} = 0 \quad \wedge \quad V_r^{\mathsf{r}} \ge 0. \tag{17}$$

We consider the following explicit constraints.

– The power flow equations state that, at each bus $b \in B$, the sum of complex injected powers S_{bah} at bus b, plus the power demand $\tilde{S}_b$ at b, is equal to the power generated by any generators installed at b, plus the shunt admittance term:

$$\forall b \in B \quad \sum_{(b,a,h) \in L} S_{bah} + \tilde{S}_b = -A_b^* |V_b|^2 + \sum_{g \in \mathscr{G}_b} \mathscr{S}_g. \tag{18}$$

As regards shunt admittance, we remark that $-A_b^* = -A_b^{\mathsf{r}} + i A_b^{\mathsf{c}}$. The shunt admittance $-A_b^* |V_b|^2$ arises when considering the line equations in Bienstock (2016, Eq. (1.10)–(1.11)) applied to a fictitious line between a bus representing the ground (with associated zero voltage magnitude) and the bus b. In particular, it can be derived from Bienstock (2016, Eq. (1.12)) by setting the voltage at the "to" node (called V_m in the cited equation) to zero.

– The definition of power in terms of current is:

$$\forall (b,a,h) \in L \quad S_{bah} = V_b\, I_{bah}^*. \tag{19}$$

– The generalized Ohm's law, which relates current to voltage, is as follows:

$$\forall (b, a, h) \in L_0 \quad I_{bah} = Y^{\mathsf{ff}}_{bah} V_b + Y^{\mathsf{ft}}_{bah} V_a \tag{20}$$

$$\forall (b, a, h) \in L_0 \quad I_{abh} = Y^{\mathsf{tf}}_{bah} V_b + Y^{\mathsf{tt}}_{bah} V_a. \tag{21}$$

4.2 A modelling issue with the power flow equations

We can now provide a deeper analysis of the second modelling issue presented in Sect. 3.1. The first term of Eq. (18) is the sum

$$\sum_{(b,a,h)\in L} S_{bah},$$

where b is fixed by the quantifier $\forall b \in B$, and the sum ranges over all a, h such that $(b, a, h) \in L$. Since L is partitioned into L_0 and L_1 as explained in Sect. 4.1.1, some indices of terms in the sum might be arcs $(b, a, h) \in L_0$ and some others might be in L_1. Moreover, no pair of antiparallel arc can ever appear in the same sum. Hence, terms S_{bah} with indices in L_0 correspond to currents I_{bah} that transform to voltage by means of the first row $(Y^{\mathsf{ff}}_{ba}, Y^{\mathsf{ft}}_{ba})$ of $\mathbf{Y}_{ba}$, while terms S_{bah} with indices in L_1 correspond to currents I_{bah} that transform to voltage by means of the second row $(Y^{\mathsf{tf}}_{ab}, Y^{\mathsf{tt}}_{ab})$ of $\mathbf{Y}_{ab}$.

The example in Fig. 2 shows a bus $b \in B$ with an adjacent neighbourhood $\{a_1, a_2, a_3\} \subset B$. Each line is represented by two anti-parallel arcs; there are no parallel lines, so we can dispense with the index h. We assume that (a_1, b), (b, a_2), (b, a_3), drawn in black in Fig. 2, are in L_0; the anti-parallel arcs (b, a_1), (a_2, b), (a_3, b), drawn in dashed grey, are in L_1. The sum above is centered in b, so it works out to $S_{ba_1} + S_{ba_2} + S_{ba_3}$; the terms in the sum are indexed by thick arcs in Fig. 2. The corresponding constraints in Eq. (19) are:

$$\begin{aligned} S_{ba_1} &= V_b \, {I_{ba_1}}^* \\ S_{ba_2} &= V_b \, {I_{ba_2}}^* \\ S_{ba_3} &= V_b \, {I_{ba_3}}^*. \end{aligned}$$

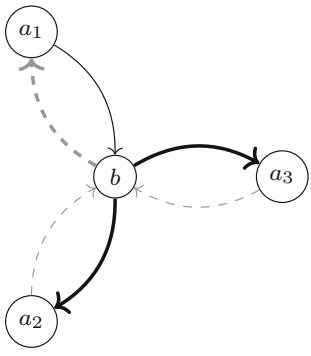

Fig. 2 Example showing how the rows of $\mathbf{Y}$ matrices apply to terms in the sum of the power flow equations

The corresponding constraints in Eqs. (20) and (21) are:

$$I_{ba_1} = Y^{\mathsf{tf}}_{a_1 b} V_{a_1} + Y^{\mathsf{tt}}_{a_1 b} V_b$$
$$I_{ba_2} = Y^{\mathsf{ff}}_{ba_2} V_b + Y^{\mathsf{ft}}_{ba_2} V_{a_2}$$
$$I_{ba_3} = Y^{\mathsf{ff}}_{ba_3} V_b + Y^{\mathsf{ft}}_{ba_3} V_{a_3}.$$

In particular, note the asymmetry between the definition of I_{ba_1} and those of I_{ba_2}, I_{ba_3}. This asymmetry is not clearly apparent in the variable indexing in the power flow equations Eq. (18), so it may lead to modelling mistakes.

This modelling issue can be addressed by separating the sum into two sums, one over L_0 and the other over L_1, so that the first sum behaves according to Eq. (20) while the second to Eq. (21) reindexed so that the bus close to the transformer is called a:

$$\forall (b, a, h) \in L_1 \quad I_{bah} = Y^{\mathsf{tf}}_{abh} V_a + Y^{\mathsf{tt}}_{abh} V_b. \tag{22}$$

We remark that the values in the matrix $\mathbf{Y}_{bah}$ in Eq. (21) are the very same values in the matrix $\mathbf{Y}_{abh}$ in Eq. (22). Finally, the relevant reformulation of Eq. (18) is:

$$\forall b \in B \quad \sum_{(b,a,h)\in L_0} S_{bah} + \sum_{(b,a,h)\in L_1} S_{bah} + \tilde{S}_b = -A_b^* |V_b|^2 + \sum_{g\in\mathscr{G}_b} \mathscr{S}_g. \tag{23}$$

4.3 Voltage-only formulation

This formulation is obtained from the (S, I, V)-formulation in Eqs. (11)–(21) by replacing injected power variables S by voltage and current variables using Eq. (19), and then all current variables I using Eqs. (20) and (21). Instead of the power flow equations in form Eq. (18) we use Eq. (23) according to the discussion in Sect. 4.2. Although this formulation is known as "voltage-only", it has two types of variables: voltage V and generated power $\mathscr{S}$. In all of this section, it is important to recall that $\bar{S}_{bah} = \bar{S}_{abh}$.

By simple substitution using Eq. (20) and (22) followed by Eq. (19), and recalling that $\forall x, y \in \mathbb{C}$ $(x + y)^* = x^* + y^*$ and $(xy)^* = x^* y^*$, we have:

$$\forall (b, a, h) \in L_0 \quad S_{bah} = Y^{\mathsf{ff}\,*}_{bah} |V_b|^2 + Y^{\mathsf{ft}\,*}_{bah} V_b V_a^* \tag{24}$$
$$\forall (b, a, h) \in L_1 \quad S_{bah} = Y^{\mathsf{tf}\,*}_{abh} V_b V_a^* + Y^{\mathsf{tt}\,*}_{abh} |V_b|^2. \tag{25}$$

Carrying out the replacements Eqs. (24) and (25) for S in terms of V in Eqs. (11)–(18) yields the MP formulation below:

$$
\left.
\begin{array}{rr}
\min & \sum_{g\in\mathscr{G}} (c_{g1}\mathscr{S}^{\mathsf{r}}_g + c_{g0}) \\
\forall b \in B, g \in \mathscr{G}_b & \underline{\mathscr{S}}_g \le \mathscr{S}_g \le \overline{\mathscr{S}}_g \\
\forall (b,a,h) \in L_0 & |\, Y^{\mathsf{ff}}_{bah}{}^* |V_b|^2 + Y^{\mathsf{ft}}_{bah}{}^* V_b\, V_a^*| \le \bar{S}_{bah} \\
\forall (b,a,h) \in L_1 & |\, Y^{\mathsf{tf}}_{abh}{}^* V_b\, V_a^* + Y^{\mathsf{tt}}_{abh}{}^* |V_b|^2| \le \bar{S}_{bah} \\
\forall (b,a,h) \in L_0 & [\tan(\underline{\eta}_{bah}), \tan(\overline{\eta}_{bah})](V_b\, V_a^*)^{\mathsf{r}} \ni (V_b\, V_a^*)^{\mathsf{c}} \\
\forall (b,a,1) \in L_0 & (V_b\, V_a^*)^{\mathsf{r}} \ge 0 \\
\forall b \in B & \underline{V}_b^2 \le |V_b|^2 \le \overline{V}_b^2 \\
 & V_r^{\mathsf{c}} = 0 \quad \wedge \quad V_r^{\mathsf{r}} \ge 0 \\
\forall b \in B & \sum_{(b,a,h)\in L_0} (Y^{\mathsf{ff}}_{bah}{}^* |V_b|^2 + Y^{\mathsf{ft}}_{bah}{}^* V_b\, V_a^*) \\
 & + \sum_{(b,a,h)\in L_1} (Y^{\mathsf{tf}}_{abh}{}^* V_b\, V_a^* + Y^{\mathsf{tt}}_{abh}{}^* |V_b|^2) \\
 & + \tilde{S}_b = -A_b^* |V_b|^2 + \sum_{g\in\mathscr{G}_b} \mathscr{S}_g .
\end{array}
\right\} \quad (26)
$$

The constraints of Eq. (26) follow the order given in Eqs. (11)–(18): generated power bounds, upper bounds on injected power, phase difference bounds, voltage magnitude bounds, reference bus bounds, and power flow equations.

Equation (26) is not quite a complex QCQP: the injected power bounds Eq. (13) either yield quartic polynomials in voltage, or the modulus of power, involving a square root. In order to obtain a complex QCQP we need to replace these constraints with corresponding constraints on the current magnitude: we replace $|S_{bah}| \le \bar{S}_{bah}$ with $|I_{bah}|^2 \le \bar{I}^2_{bah}$ over all $(b,a,h) \in L_0$ (and correspondingly for L_1). After replacing I_{bah} with the corresponding voltage terms according to Ohm's law, we obtain the following:

$$\forall (b,a,h) \in L_0 \quad |Y^{\mathsf{ff}}_{bah} V_b + Y^{\mathsf{ft}}_{bah} V_a|^2 \le \bar{I}^2_{bah} \quad (27)$$

$$\forall (b,a,h) \in L_1 \quad |Y^{\mathsf{tf}}_{abh} V_a + Y^{\mathsf{tt}}_{abh} V_b|^2 \le \bar{I}^2_{bah}. \quad (28)$$

Note that Eqs. (27) and (28) are quadratic in V, as required.

Technically speaking, there is no loss of information or precision in replacing power magnitude bounds with current magnitude bounds, since upper bounds to injected power are often derived from upper bounds to current on the same line. On the other hand, the actual data for $\bar{I}$ may not be given. In this case we can form the relaxation given by replacing the injected power bound constraints in Eq. (26) with:

$$\forall (b,a,h) \in L_0 \quad |Y^{\mathsf{ff}}_{bah} V_b + Y^{\mathsf{ft}}_{bah} V_a|^2 \le \bar{S}^2_{bah}/\underline{V}^2_b \quad (29)$$

$$\forall (b,a,h) \in L_1 \quad |Y^{\mathsf{tf}}_{abh} V_a + Y^{\mathsf{tt}}_{abh} V_b|^2 \le \bar{S}^2_{bah}/\underline{V}^2_b. \quad (30)$$

Equations (29) and (30) are valid constraints for Eq. (26) because:

$$\underline{V}_b \le |V_b| \Rightarrow \underline{V}_b |I_{bah}| \le |V_b|\,|I_{bah}| \Rightarrow \underline{V}_b |I_{bah}| \le \\ \le |V_b|\,|\,I_{bah}{}^*| = |V_b\, I_{bah}{}^*| = |S_{bah}| \le \bar{S}_{bah}$$

for all $(b, a, h) \in L_0$, whence $|I_{bah}| \le \bar{S}_{bah}/\underline{V}_b$. The argument for $(b, a, h) \in L_1$ is similar (note that $|xy| = |x|\,|y|$ for $x, y \in \mathbb{C}$). Hence Eqs. (29) and (30) provide a relaxation of Eq. (26), as claimed. Note that Eqs. (29) and (30) are quadratic in V, so this relaxation is also a complex QCQP.

4.4 Semidefinite relaxation

We derive a complex Semidefinite Programming (SDP) relaxation from the complex QCQP arising from Eq. (26), and using the current magnitude bound constraints Eqs. (27) and (28). For each $(b, a, h) \in L_0$ we have:

$$\begin{aligned}
&|Y^{\mathsf{ff}}_{bah} V_b + Y^{\mathsf{ft}}_{bah} V_a|^2 \\
&= (Y^{\mathsf{ff}}_{bah} V_b + Y^{\mathsf{ft}}_{bah} V_a)\,(Y^{\mathsf{ff}}_{bah} V_b + Y^{\mathsf{ft}}_{bah} V_a)^* \\
&= (Y^{\mathsf{ff}}_{bah} V_b + Y^{\mathsf{ft}}_{bah} V_a)(\,Y^{\mathsf{ff}}_{bah}{}^* V_b^* + Y^{\mathsf{ft}}_{bah}{}^* V_a^*) \\
&= |Y^{\mathsf{ff}}_{bah}|^2 |V_b|^2 + |Y^{\mathsf{ft}}_{bah}|^2 |V_a|^2 + Y^{\mathsf{ff}}_{bah}\, Y^{\mathsf{ft}}_{bah}{}^* V_b\, V_a^* + Y^{\mathsf{ff}}_{bah}{}^* Y^{\mathsf{ft}}_{bah}\, V_b^* V_a \\
&= |Y^{\mathsf{ff}}_{bah}|^2 |V_b|^2 + |Y^{\mathsf{ft}}_{bah}|^2 |V_a|^2 + Y^{\mathsf{ff}}_{bah}\, Y^{\mathsf{ft}}_{bah}{}^* V_b\, V_a^* + (Y^{\mathsf{ff}}_{bah}\, Y^{\mathsf{ft}}_{bah}{}^*)^*\,(V_b\, V_a^*)^* \\
&= |Y^{\mathsf{ff}}_{bah}|^2 |V_b|^2 + |Y^{\mathsf{ft}}_{bah}|^2 |V_a|^2 + Y^{\mathsf{ff}}_{bah}\, Y^{\mathsf{ft}}_{bah}{}^* V_b\, V_a^* + (Y^{\mathsf{ff}}_{bah}\, Y^{\mathsf{ft}}_{bah}{}^* V_b\, V_a^*)^* \\
&= |Y^{\mathsf{ff}}_{bah}|^2 |V_b|^2 + |Y^{\mathsf{ft}}_{bah}|^2 |V_a|^2 + 2(Y^{\mathsf{ff}}_{bah}\, Y^{\mathsf{ft}}_{bah}{}^* V_b\, V_a^*)^{\mathsf{r}}.
\end{aligned}$$

Similarly, for each $(b, a, h) \in L_1$ we have:

$$\begin{aligned}
&|Y^{\mathsf{tf}}_{abh} V_a + Y^{\mathsf{tt}}_{abh} V_b|^2 \\
&= |Y^{\mathsf{tf}}_{abh}|^2 |V_a|^2 + |Y^{\mathsf{tt}}_{abh}|^2 |V_b|^2 + (Y^{\mathsf{tf}}_{abh}\, Y^{\mathsf{tt}}_{abh}{}^* V_a\, V_b^*) + (\,Y^{\mathsf{tf}}_{abh}{}^* Y^{\mathsf{tt}}_{abh}\, V_a^* V_b) \\
&= |Y^{\mathsf{tf}}_{abh}|^2 |V_a|^2 + |Y^{\mathsf{tt}}_{abh}|^2 |V_b|^2 + 2(Y^{\mathsf{tf}}_{abh}\, Y^{\mathsf{tt}}_{abh}{}^* V_a\, V_b^*)^{\mathsf{r}}.
\end{aligned}$$

We then rewrite Eq. (26) as a complex QCQP as follows, where the terms for the squared current modulus have been further modified via Eqs. (3) and (4).

$$
\left.
\begin{array}{rr}
\min & \sum_{g\in\mathscr{G}} (c_{g1}\mathscr{S}_g^{\mathsf{r}} + c_{g0}) \\
\forall b \in B, g \in \mathscr{G}_b & \underline{\mathscr{S}}_g \le \mathscr{S}_g \le \overline{\mathscr{S}}_g \\
\forall (b,a,h) \in L_0 & |Y_{bah}^{\mathsf{ff}}|^2 |V_b|^2 + |Y_{bah}^{\mathsf{ft}}|^2 |V_a|^2 \\
& + Y_{bah}^{\mathsf{ff}}\, Y_{bah}^{\mathsf{ft}\,*} V_b\, V_a^* + Y_{bah}^{\mathsf{ff}\,*} Y_{bah}^{\mathsf{ft}}\, V_a\, V_b^* \le \bar{I}_{bah}^2 \\
\forall (b,a,h) \in L_1 & |Y_{abh}^{\mathsf{tf}}|^2 |V_a|^2 + |Y_{abh}^{\mathsf{tt}}|^2 |V_b|^2 \\
& + Y_{abh}^{\mathsf{tf}}\, Y_{abh}^{\mathsf{tt}\,*} V_a\, V_b^* + Y_{abh}^{\mathsf{tf}\,*} Y_{abh}^{\mathsf{tt}}\, V_b\, V_a^* \le \bar{I}_{bah}^2 \\
\forall (b,a,h) \in L_0 & (\tan(\underline{\eta}_{bah}) + i) V_b\, V_a^* + (\tan(\underline{\eta}_{bah}) - i) V_a\, V_b^* \le 0 \\
\forall (b,a,h) \in L_0 & (\tan(\overline{\eta}_{bah}) + i) V_b\, V_a^* + (\tan(\overline{\eta}_{bah}) - i) V_a\, V_b^* \ge 0 \\
\forall (b,a,1) \in L_0 & (V_b\, V_a^* + V_a\, V_b^*) \ge 0 \\
\forall b \in B & \underline{V}_b^2 \le |V_b|^2 \le \overline{V}_b^2 \\
& V_r - V_r^* = 0 \quad \wedge \quad V_r + V_r^* \ge 0 \\
\forall b \in B & \sum_{(b,a,h)\in L_0} (Y_{bah}^{\mathsf{ff}\,*} |V_b|^2 + Y_{bah}^{\mathsf{ft}\,*} V_b\, V_a^*) \\
& + \sum_{(b,a,h)\in L_1} (Y_{abh}^{\mathsf{tf}\,*} V_b\, V_a^* + Y_{abh}^{\mathsf{tt}\,*} |V_b|^2) \\
& + \tilde{S}_b = -A_b^* |V_b|^2 + \sum_{g\in\mathscr{G}_b} \mathscr{S}_g,
\end{array}
\right\} \quad (31)
$$

so that the voltage appears linearly only as V_r, and quadratically as $|V_b|^2$, $V_b\, V_a^*$, and $(V_b\, V_a^*)^* = V_a\, V_b^*$. We remark that the phase difference bound inequalities in Eq. (31) (involving tangents) follow from Eqs. (3) and (4).

We now form a matrix of n^2 decision variables products, which we linearize by using a Hermitian matrix X:

$$
V V^{\mathsf{H}} = \begin{pmatrix} |V_1|^2 & V_1\, V_2^* & \cdots & V_1\, V_n^* \\ V_2\, V_1^* & |V_2|^2 & \cdots & V_2\, V_n^* \\ \vdots & \vdots & \ddots & \vdots \\ V_n\, V_1^* & V_n\, V_2^* & \cdots & |V_n|^2 \end{pmatrix} = \begin{pmatrix} X_{11} & X_{12} & \cdots & X_{1n} \\ X_{21} & X_{22} & \cdots & X_{2n} \\ \vdots & \vdots & \ddots & \vdots \\ X_{n1} & X_{n2} & \cdots & X_{nn} \end{pmatrix} = X.
$$

This directly leads to a complex SDP relaxation of the ACOPF, which consists in relaxing $X = V V^{\mathsf{H}}$ to

$$
X \succeq_{\mathsf{H}} V V^{\mathsf{H}}, \quad (32)
$$

where $\succeq_{\mathsf{H}}$ denotes the Loewner order on Hermitian matrices: two Hermitian matrices A, B are in the order $A \succeq_H B$ if $A - B$ is positive semidefinite (PSD). This order naturally restricts to the familiar order $A \succeq B$ to mean $A - B$ is PSD on real matrices A, B. The formulation is as follows:

$$
\left.
\begin{array}{rrcl}
\min & \sum_{g\in\mathscr{G}} (c_{g1}\mathscr{S}_g^{\mathsf{r}} + c_{g0}) & & \\
\forall b \in B, g \in \mathscr{G}_b & \underline{\mathscr{S}}_g \le \mathscr{S}_g & \le & \overline{\mathscr{S}}_g \\
\forall (b,a,h) \in L_0 & |Y_{bah}^{\mathsf{ff}}|^2 X_{bb} + |Y_{bah}^{\mathsf{ft}}|^2 X_{aa} & & \\
& + Y_{bah}^{\mathsf{ff}}\, Y_{bah}^{\mathsf{ft}}{}^{*} X_{ba} + Y_{bah}^{\mathsf{ff}}{}^{*} Y_{bah}^{\mathsf{ft}} X_{ab} & \le & \bar{I}_{bah}^2 \\
\forall (b,a,h) \in L_1 & |Y_{abh}^{\mathsf{tf}}|^2 X_{aa} + |Y_{abh}^{\mathsf{tt}}|^2 X_{bb} & & \\
& + Y_{abh}^{\mathsf{tf}}\, Y_{abh}^{\mathsf{tt}}{}^{*} X_{ab} + Y_{abh}^{\mathsf{tf}}{}^{*} Y_{abh}^{\mathsf{tt}} X_{ba} & \le & \bar{I}_{bah}^2 \\
\forall (b,a,h) \in L_0 & (\tan(\underline{\eta}_{bah}) + i) X_{ba} + (\tan(\underline{\eta}_{bah}) - i) X_{ab} & \le & 0 \\
\forall (b,a,h) \in L_0 & (\tan(\overline{\eta}_{bah}) + i) X_{ba} + (\tan(\overline{\eta}_{bah}) - i) X_{ab} & \ge & 0 \\
\forall (b,a,1) \in L_0 & (X_{ba} + X_{ab}) & \ge & 0 \\
\forall b \in B & \underline{V}_b^2 \le X_{bb} & \le & \overline{V}_b^2 \\
& V_r - V_r^* = 0 \quad \wedge \quad V_r + V_r^* & \ge & 0 \\
\forall b \in B & \sum_{(b,a,h)\in L_0} (Y_{bah}^{\mathsf{ff}}{}^{*} X_{bb} + Y_{bah}^{\mathsf{ft}}{}^{*} X_{ba}) & & \\
& + \sum_{(b,a,h)\in L_1} (Y_{abh}^{\mathsf{tf}}{}^{*} X_{ba} + Y_{abh}^{\mathsf{tt}}{}^{*} X_{bb}) & & \\
& + \tilde{S}_b = - A_b{}^{*} X_{bb} + \sum_{g\in\mathscr{G}_b} \mathscr{S}_g & & \\
& \begin{pmatrix} 1 & V^{\mathsf{H}} \\ V & X \end{pmatrix} \succeq_{\mathsf{H}} 0. &&
\end{array}
\right\} \quad (33)
$$

The last constraint in Eq. (33) is derived from Eq. (32) using the Schur complement.

A complex SDP relaxation (widely used in the literature) is obtained by relaxing the reference bus constraint and bounding the injected power on lines instead of the current on lines. The decision variables of this formulation are the matrix X and the flow variables S_{bah} (for $(b,a,h) \in L$). The formulation is as follows:

$$
\left.
\begin{array}{rrcl}
\min & \sum_{g\in\mathscr{G}} (c_{g1}\mathscr{S}_g^{\mathsf{r}} + c_{g0}) & & \\
\forall b \in B, g \in \mathscr{G}_b & \underline{\mathscr{S}}_g \le \mathscr{S}_g & \le & \overline{\mathscr{S}}_g \\
\forall (b,a,h) \in L_0 & Y_{bah}^{\mathsf{ff}}{}^{*} X_{bb} + Y_{bah}^{\mathsf{ft}}{}^{*} X_{ba} & = & S_{bah} \\
\forall (b,a,h) \in L_1 & Y_{abh}^{\mathsf{tf}}{}^{*} X_{ba} + Y_{abh}^{\mathsf{tt}}{}^{*} X_{bb} & = & S_{bah} \\
\forall (b,a,h) \in L & S_{bah}\, S_{bah}^{*} & \le & \overline{S}_{bah}^2 \\
\forall (b,a,h) \in L_0 & (\tan(\underline{\eta}_{bah}) + i) X_{ba} + (\tan(\underline{\eta}_{bah}) - i) X_{ab} & \le & 0 \\
\forall (b,a,h) \in L_0 & (\tan(\overline{\eta}_{bah}) + i) X_{ba} + (\tan(\overline{\eta}_{bah}) - i) X_{ab} & \ge & 0 \\
\forall (b,a,1) \in L_0 & (X_{ba} + X_{ab}) & \ge & 0 \\
\forall b \in B & \underline{V}_b^2 \le X_{bb} & \le & \overline{V}_b^2 \\
\forall b \in B & \sum_{(b,a,h)\in L} S_{bah} + \tilde{S}_b + A_b{}^{*} X_{bb} - \sum_{g\in\mathscr{G}_b} \mathscr{S}_g & = & 0 \\
& X \succeq_{\mathsf{H}} 0. &&
\end{array}
\right\} \quad (34)
$$

We note that the PSD constraint $X \succeq_{\mathsf{H}} 0$ is equivalent to Eq. (32) for Eq. (34) because the V variables do not appear therein.

5 Real formulations

In this section we shall explain how to obtain real number formulations from the formulations in complex numbers discussed in Sect. 4.

5.1 Cartesian (*S*, *I*, *V*)-formulation

This formulation is obtained by separating real and imaginary parts of decision variables and constraints in the complex (S, I, V)-formulation from Sect. 4.1. Decision variables are dealt with as follows:

$$\begin{aligned}
\forall b \in B \quad & V_b = {V_b}^{\mathsf{r}} + i\,{V_b}^{\mathsf{c}} \\
\forall (b,a,h) \in L \quad & I_b = {I_{bah}}^{\mathsf{r}} + i\,{I_{bah}}^{\mathsf{c}} \\
\forall (b,a,h) \in L \quad & S_b = {S_{bah}}^{\mathsf{r}} + i\,{S_{bah}}^{\mathsf{c}} \\
\forall g \in \mathscr{G} \quad & \mathscr{S}_g = {\mathscr{S}_g}^{\mathsf{r}} + i\,{\mathscr{S}_g}^{\mathsf{c}}.
\end{aligned}$$

As mentioned in Sect. 4.1, the objective function is assumed to be real. We now tackle the constraints:

– Generated power bounds Eq. (12):

$$\forall g \in \mathscr{G} \quad {\underline{\mathscr{S}}_g}^{\mathsf{r}} \le {\mathscr{S}_g}^{\mathsf{r}} \le {\overline{\mathscr{S}}_g}^{\mathsf{r}} \tag{35}$$

$$\forall g \in \mathscr{G} \quad {\underline{\mathscr{S}}_g}^{\mathsf{c}} \le {\mathscr{S}_g}^{\mathsf{c}} \le {\overline{\mathscr{S}}_g}^{\mathsf{c}}. \tag{36}$$

– Bounds on the power magnitude Eq. (13):

$$\forall (b,a,h) \in L \quad ({S_{bah}}^{\mathsf{r}})^2 + ({S_{bah}}^{\mathsf{c}})^2 \le \bar{S}_{bah}^2. \tag{37}$$

– Bounds on phase differences Eqs. (14) and (15):

$$\forall (b,a,h) \in L_0 \quad \tan(\underline{\eta}_{bah})({V_b}^{\mathsf{r}}{V_a}^{\mathsf{r}} + {V_b}^{\mathsf{c}}{V_a}^{\mathsf{c}}) \le {V_b}^{\mathsf{c}}{V_a}^{\mathsf{r}} - {V_b}^{\mathsf{r}}{V_a}^{\mathsf{c}} \tag{38}$$

$$\forall (b,a,h) \in L_0 \quad {V_b}^{\mathsf{c}}{V_a}^{\mathsf{r}} - {V_b}^{\mathsf{r}}{V_a}^{\mathsf{c}} \le \tan(\overline{\eta}_{bah})({V_b}^{\mathsf{r}}{V_a}^{\mathsf{r}} + {V_b}^{\mathsf{c}}{V_a}^{\mathsf{c}}) \tag{39}$$

$$\forall (b,a,1) \in L_0 \quad {V_b}^{\mathsf{r}}{V_a}^{\mathsf{r}} + {V_b}^{\mathsf{c}}{V_a}^{\mathsf{c}} \ge 0. \tag{40}$$

– Voltage bounds Eq. (16):

$$\forall b \in B \quad \underline{V}_b^2 \le ({V_b}^{\mathsf{r}})^2 + ({V_b}^{\mathsf{c}})^2 \le \overline{V}_b^2. \tag{41}$$

– The reference bus constraints Eq. (17) are unchanged.

– Power flow equations Eq. (18):

$$\forall b \in B \quad \sum_{(b,a,h)\in L} (S_{bah})^{\mathsf{r}} + \tilde{S}_b^{\mathsf{r}} = -A_b{}^{\mathsf{r}}|V_b|^2 + \sum_{g\in\mathscr{G}_b} \mathscr{S}_g{}^{\mathsf{r}} \tag{42}$$

$$\forall b \in B \quad \sum_{(b,a,h)\in L} (S_{bah})^{\mathsf{c}} + \tilde{S}_b^{\mathsf{c}} = A_b{}^{\mathsf{c}}|V_b|^2 + \sum_{g\in\mathscr{G}_b} \mathscr{S}_g{}^{\mathsf{c}}. \tag{43}$$

– Power in terms of current Eq. (19):

$$\forall (b,a,h) \in L \quad (S_{bah})^{\mathsf{r}} = V_b{}^{\mathsf{r}}(I_{bah})^{\mathsf{r}} + V_b{}^{\mathsf{c}}(I_{bah})^{\mathsf{c}} \tag{44}$$

$$\forall (b,a,h) \in L \quad (S_{bah})^{\mathsf{c}} = V_b{}^{\mathsf{c}}(I_{bah})^{\mathsf{r}} - V_b{}^{\mathsf{r}}(I_{bah})^{\mathsf{c}}. \tag{45}$$

– Generalized Ohm's law Eqs. (20) and (21):

$$\forall (b,a,h) \in L_0 \quad I_{bah}{}^{\mathsf{r}} = (Y_{bah}^{\mathsf{ff}})^{\mathsf{r}} V_b{}^{\mathsf{r}} - (Y_{bah}^{\mathsf{ff}})^{\mathsf{c}} V_b{}^{\mathsf{c}} + (Y_{bah}^{\mathsf{ft}})^{\mathsf{r}} V_a{}^{\mathsf{r}} - (Y_{bah}^{\mathsf{ft}})^{\mathsf{c}} V_a{}^{\mathsf{c}} \tag{46}$$

$$\forall (b,a,h) \in L_0 \quad I_{bah}{}^{\mathsf{c}} = (Y_{bah}^{\mathsf{ff}})^{\mathsf{r}} V_b{}^{\mathsf{c}} + (Y_{bah}^{\mathsf{ff}})^{\mathsf{c}} V_b{}^{\mathsf{r}} + (Y_{bah}^{\mathsf{ft}})^{\mathsf{r}} V_a{}^{\mathsf{c}} + (Y_{bah}^{\mathsf{ft}})^{\mathsf{c}} V_a{}^{\mathsf{r}} \tag{47}$$

$$\forall (b,a,h) \in L_0 \quad I_{abh}{}^{\mathsf{r}} = (Y_{bah}^{\mathsf{tf}})^{\mathsf{r}} V_b{}^{\mathsf{r}} - (Y_{bah}^{\mathsf{tf}})^{\mathsf{c}} V_b{}^{\mathsf{c}} + (Y_{bah}^{\mathsf{tt}})^{\mathsf{r}} V_a{}^{\mathsf{r}} - (Y_{bah}^{\mathsf{tt}})^{\mathsf{c}} V_a{}^{\mathsf{c}} \tag{48}$$

$$\forall (b,a,h) \in L_0 \quad I_{abh}{}^{\mathsf{c}} = (Y_{bah}^{\mathsf{tf}})^{\mathsf{r}} V_b{}^{\mathsf{c}} + (Y_{bah}^{\mathsf{tf}})^{\mathsf{c}} V_b{}^{\mathsf{r}} + (Y_{bah}^{\mathsf{tt}})^{\mathsf{r}} V_a{}^{\mathsf{c}} + (Y_{bah}^{\mathsf{tt}})^{\mathsf{c}} V_a{}^{\mathsf{r}} \tag{49}$$

5.2 Cartesian voltage-only QCQP

This formulation is derived from Eq. (31); as such, it relies on magnitude bounds $\bar{I}$ on injected current rather than magnitude bounds $\bar{S}$ on injected power.

The objective function, linear in active power, is already a real function of real variables only. The bounds on generated power are enforced on real and complex parts separately, as in Eqs. (35) and (36). We separate real and imaginary parts of the terms in the current magnitude bounds in Eqs. (27) and (28), and obtain:

$$\forall (b,a,h) \in L_0 \quad |Y_{bah}^{\mathsf{ff}}|^2|V_b|^2 + |Y_{bah}^{\mathsf{ft}}|^2|V_a|^2 + 2(Y_{bah}^{\mathsf{ff}}\, Y_{bah}^{\mathsf{ft}\,*} V_b\, V_a^*)^{\mathsf{r}} \le \bar{I}_{bah}^2 \tag{50}$$

$$\forall (b,a,h) \in L_1 \quad |Y_{abh}^{\mathsf{tf}}|^2|V_a|^2 + |Y_{abh}^{\mathsf{tt}}|^2|V_b|^2 + 2(Y_{abh}^{\mathsf{tf}}\, Y_{abh}^{\mathsf{tt}\,*} V_a\, V_b^*)^{\mathsf{r}} \le \bar{I}_{bah}^2, \tag{51}$$

where

$$|V_b|^2 = (V_b{}^{\mathsf{r}})^2 + (V_b{}^{\mathsf{c}})^2 \quad \wedge \quad |V_a|^2 = (V_a{}^{\mathsf{r}})^2 + (V_a{}^{\mathsf{c}})^2 \tag{52}$$

$$\begin{aligned}(Y_{bah}^{\mathsf{ff}}\, Y_{bah}^{\mathsf{ft}\,*} V_b\, V_a^*)^{\mathsf{r}} &= Y_{bah}^{\mathsf{ff}}{}^{\mathsf{r}} Y_{bah}^{\mathsf{ft}}{}^{\mathsf{r}} V_b{}^{\mathsf{r}} V_a{}^{\mathsf{r}} + Y_{bah}^{\mathsf{ff}}{}^{\mathsf{c}} Y_{bah}^{\mathsf{ft}}{}^{\mathsf{c}} V_b{}^{\mathsf{c}} V_a{}^{\mathsf{c}} + Y_{bah}^{\mathsf{ff}}{}^{\mathsf{r}} Y_{bah}^{\mathsf{ft}}{}^{\mathsf{r}} V_b{}^{\mathsf{c}} V_a{}^{\mathsf{c}} + Y_{bah}^{\mathsf{ff}}{}^{\mathsf{c}} Y_{bah}^{\mathsf{ft}}{}^{\mathsf{c}} V_b{}^{\mathsf{r}} V_a{}^{\mathsf{r}} \\ &\quad - Y_{bah}^{\mathsf{ff}}{}^{\mathsf{r}} Y_{bah}^{\mathsf{ft}}{}^{\mathsf{c}} V_b{}^{\mathsf{r}} V_a{}^{\mathsf{c}} - Y_{bah}^{\mathsf{ff}}{}^{\mathsf{c}} Y_{bah}^{\mathsf{ft}}{}^{\mathsf{r}} V_b{}^{\mathsf{c}} V_a{}^{\mathsf{r}} + Y_{bah}^{\mathsf{ff}}{}^{\mathsf{r}} Y_{bah}^{\mathsf{ft}}{}^{\mathsf{c}} V_b{}^{\mathsf{c}} V_a{}^{\mathsf{r}} + Y_{bah}^{\mathsf{ff}}{}^{\mathsf{c}} Y_{bah}^{\mathsf{ft}}{}^{\mathsf{r}} V_b{}^{\mathsf{r}} V_a{}^{\mathsf{c}}\end{aligned} \tag{53}$$

$$\begin{aligned}(Y_{abh}^{\mathsf{tf}}\, Y_{abh}^{\mathsf{tt}\,*} V_a\, V_b^*)^{\mathsf{r}} &= Y_{abh}^{\mathsf{tf}}{}^{\mathsf{r}} Y_{abh}^{\mathsf{tt}}{}^{\mathsf{r}} V_a{}^{\mathsf{r}} V_b{}^{\mathsf{r}} + Y_{abh}^{\mathsf{tf}}{}^{\mathsf{c}} Y_{abh}^{\mathsf{tt}}{}^{\mathsf{c}} V_a{}^{\mathsf{c}} V_b{}^{\mathsf{c}} + Y_{abh}^{\mathsf{tf}}{}^{\mathsf{r}} Y_{abh}^{\mathsf{tt}}{}^{\mathsf{r}} V_a{}^{\mathsf{c}} V_b{}^{\mathsf{c}} + Y_{abh}^{\mathsf{tf}}{}^{\mathsf{c}} Y_{abh}^{\mathsf{tt}}{}^{\mathsf{c}} V_a{}^{\mathsf{r}} V_b{}^{\mathsf{r}} \\ &\quad - Y_{abh}^{\mathsf{tf}}{}^{\mathsf{r}} Y_{abh}^{\mathsf{tt}}{}^{\mathsf{c}} V_a{}^{\mathsf{r}} V_b{}^{\mathsf{c}} - Y_{abh}^{\mathsf{tf}}{}^{\mathsf{c}} Y_{abh}^{\mathsf{tt}}{}^{\mathsf{r}} V_a{}^{\mathsf{c}} V_b{}^{\mathsf{r}} + Y_{abh}^{\mathsf{tf}}{}^{\mathsf{r}} Y_{abh}^{\mathsf{tt}}{}^{\mathsf{c}} V_a{}^{\mathsf{c}} V_b{}^{\mathsf{r}} + Y_{abh}^{\mathsf{tf}}{}^{\mathsf{c}} Y_{abh}^{\mathsf{tt}}{}^{\mathsf{r}} V_a{}^{\mathsf{r}} V_b{}^{\mathsf{c}}.\end{aligned} \tag{54}$$

The bounds on phase difference follow from Eq. (14) using the identities:

$$(V_b\, V_a^*)^{\mathsf{r}} = V_b{}^{\mathsf{r}} V_a{}^{\mathsf{r}} + V_b{}^{\mathsf{c}} V_a{}^{\mathsf{c}} \qquad (V_b\, V_a^*)^{\mathsf{c}} = V_b{}^{\mathsf{c}} V_a{}^{\mathsf{r}} - V_b{}^{\mathsf{r}} V_a{}^{\mathsf{c}}. \tag{55}$$

We obtain:

$$\forall (b,a,h) \in L_0 \quad \tan(\underline{\eta}_{bah})(V_b{}^{\mathsf{r}} V_a{}^{\mathsf{r}} + V_b{}^{\mathsf{c}} V_a{}^{\mathsf{c}}) \le V_b{}^{\mathsf{c}} V_a{}^{\mathsf{r}} - V_b{}^{\mathsf{r}} V_a{}^{\mathsf{c}} \tag{56}$$

$$\forall (b,a,h) \in L_0 \quad V_b{}^{\mathsf{c}} V_a{}^{\mathsf{r}} - V_b{}^{\mathsf{r}} V_a{}^{\mathsf{c}} \le \tan(\overline{\eta}_{bah})(V_b{}^{\mathsf{r}} V_a{}^{\mathsf{r}} + V_b{}^{\mathsf{c}} V_a{}^{\mathsf{c}}) \tag{57}$$

$$\forall (b,a,1) \in L_0 \quad V_b{}^{\mathsf{r}} V_a{}^{\mathsf{r}} + V_b{}^{\mathsf{c}} V_a{}^{\mathsf{c}} \ge 0. \tag{58}$$

Voltage bounds are as in Eq. (41), and reference bus constraints are as in Eq. (17).

As concerns power, we separate real and imaginary parts of the decision variables in Eqs. (24) and (25), and obtain:

$$\forall (b,a,h) \in L_0:$$

$$(S_{bah})^{\mathsf{r}} = (Y_{bah}^{\mathsf{ff}})^{\mathsf{r}} |V_b|^2 + (Y_{bah}^{\mathsf{ft}})^{\mathsf{r}} (V_b{}^{\mathsf{r}} V_a{}^{\mathsf{r}} + V_b{}^{\mathsf{c}} V_a{}^{\mathsf{c}}) + (Y_{bah}^{\mathsf{ft}})^{\mathsf{c}} (V_b{}^{\mathsf{c}} V_a{}^{\mathsf{r}} - V_b{}^{\mathsf{r}} V_a{}^{\mathsf{c}}) \tag{59}$$

$$(S_{bah})^{\mathsf{c}} = -(Y_{bah}^{\mathsf{ff}})^{\mathsf{c}} |V_b|^2 + (Y_{bah}^{\mathsf{ft}})^{\mathsf{r}} (V_b{}^{\mathsf{c}} V_a{}^{\mathsf{r}} - V_b{}^{\mathsf{r}} V_a{}^{\mathsf{c}}) - (Y_{bah}^{\mathsf{ft}})^{\mathsf{c}} (V_b{}^{\mathsf{r}} V_a{}^{\mathsf{r}} + V_b{}^{\mathsf{c}} V_a{}^{\mathsf{c}}) \tag{60}$$

$$\forall (b,a,h) \in L_1:$$

$$(S_{bah})^{\mathsf{r}} = (Y_{abh}^{\mathsf{tt}})^{\mathsf{r}} |V_b|^2 + (Y_{abh}^{\mathsf{tf}})^{\mathsf{r}} (V_b{}^{\mathsf{r}} V_a{}^{\mathsf{r}} + V_b{}^{\mathsf{c}} V_a{}^{\mathsf{c}}) + (Y_{abh}^{\mathsf{tf}})^{\mathsf{c}} (V_b{}^{\mathsf{c}} V_a{}^{\mathsf{r}} - V_b{}^{\mathsf{r}} V_a{}^{\mathsf{c}}) \tag{61}$$

$$(S_{bah})^{\mathsf{c}} = -(Y_{abh}^{\mathsf{tt}})^{\mathsf{c}} |V_b|^2 + (Y_{abh}^{\mathsf{tf}})^{\mathsf{r}} (V_b{}^{\mathsf{c}} V_a{}^{\mathsf{r}} - V_b{}^{\mathsf{r}} V_a{}^{\mathsf{c}}) - (Y_{abh}^{\mathsf{tf}})^{\mathsf{c}} (V_b{}^{\mathsf{r}} V_a{}^{\mathsf{r}} + V_b{}^{\mathsf{c}} V_a{}^{\mathsf{c}}), \tag{62}$$

which can now be replaced in Eqs. (42) and (43) when written with separate sums over L_0, L_1 as in Eq. (23).

Note that we use the generalized Ohm's laws and the power definitions in terms of current only in order to operate replacement of S_{bah} in the power flow equations Eqs. (59)–(62).

5.3 Polar formulation

The polar formulation of the ACOPF is obtained by the polar representation of complex voltage in terms of magnitude and phase:

$$\forall b \in B \quad V_b = v_b e^{i\theta_b}, \tag{63}$$

where v_b is the magnitude and θ_b is the phase (we remark that in Sect. 2 we already introduced a scaled magnitude $V_b^{\max} = v_b/\sqrt{2}$). In the current setting, v_b and θ_b are decision variables of the polar formulation. We also consider power generation variables $\mathscr{S}_g$ for $g \in \mathscr{G}$.

Since we are describing a real (rather than complex) formulation, we write:

$$\forall b \in B \quad V_b{}^{\mathsf{r}} = v_b \cos\theta_b \tag{64}$$

$$\forall b \in B \quad V_b{}^{\mathsf{c}} = v_b \sin\theta_b. \tag{65}$$

Aside from Eqs. (64) and (65), there is another implied relationship

$$\forall b \in B \quad v_b^2 = |V_b|^2, \tag{66}$$

between polar and cartesian formulations. All of these define nonconvex sets, however, so they are not exploited directly in MP formulations. By Eq. (66), however, we can derive the bound constraints:

$$\forall b \in B \quad v_b \geq 0. \tag{67}$$

Moreover, by the periodicity of trigonometric functions, we can enforce the bound constraints:

$$\forall b \in B \quad -\pi \leq \theta_b \leq \pi. \tag{68}$$

The objective function is the same as in Eq. (9). The same holds for the power generation bounds Eqs. (35) and (36). The voltage magnitude bounds are

$$\forall b \in B \quad \underline{V}_b \leq v_b \leq \overline{V}_b, \tag{69}$$

and the phase difference bounds are

$$\forall (b, a, h) \in L_0 \quad \underline{\eta}_{bah} \leq \theta_b - \theta_a \leq \overline{\eta}_{bah}. \tag{70}$$

We shall use the equations defining power in terms of current and voltage Eq. (19) and the generalized Ohm's laws in order to write the injected power bounds Eq. (13) and the power flow equations Eq. (18). We therefore have to express the injected power S on the lines in function of the polar coordinate variables v, θ. We can achieve this by replacing the right hand sides (rhs) of Eqs. (64) and (65) in the definitions of real and imaginary parts of voltage in Eqs. (59)–(62), followed by the application of Ptolemy's identities:

$$\cos(\theta_b - \theta_a) = \cos\theta_b \cos\theta_a + \sin\theta_b \sin\theta_a \tag{71}$$

$$\sin(\theta_b - \theta_a) = \sin\theta_b \cos\theta_a - \cos\theta_b \sin\theta_a. \tag{72}$$

This yields:

$$\begin{aligned}
&\forall (b, a, h) \in L_0 : \\
&\quad (S_{bah})^{\mathsf{r}} = (Y^{\mathsf{ff}}_{bah})^{\mathsf{r}} v_b^2 + (Y^{\mathsf{ft}}_{bah})^{\mathsf{r}} v_b v_a \cos(\theta_b - \theta_a) + (Y^{\mathsf{ft}}_{bah})^{\mathsf{c}} v_b v_a \sin(\theta_b - \theta_a) && (73)\\
&\quad (S_{bah})^{\mathsf{c}} = -(Y^{\mathsf{ff}}_{bah})^{\mathsf{c}} v_b^2 + (Y^{\mathsf{ft}}_{bah})^{\mathsf{r}} v_b v_a \sin(\theta_b - \theta_a) - (Y^{\mathsf{ft}}_{bah})^{\mathsf{c}} v_b v_a \cos(\theta_b - \theta_a) && (74)\\
&\forall (b, a, h) \in L_1 : \\
&\quad (S_{bah})^{\mathsf{r}} = (Y^{\mathsf{tt}}_{abh})^{\mathsf{r}} v_b^2 + (Y^{\mathsf{tf}}_{abh})^{\mathsf{r}} v_b v_a \cos(\theta_b - \theta_a) + (Y^{\mathsf{tf}}_{abh})^{\mathsf{c}} v_b v_a \sin(\theta_b - \theta_a) && (75)\\
&\quad (S_{bah})^{\mathsf{c}} = -(Y^{\mathsf{tt}}_{abh})^{\mathsf{c}} v_b^2 + (Y^{\mathsf{tf}}_{abh})^{\mathsf{r}} v_b v_a \sin(\theta_b - \theta_a) - (Y^{\mathsf{tf}}_{abh})^{\mathsf{c}} v_b v_a \cos(\theta_b - \theta_a). && (76)
\end{aligned}$$

As in Sect. 5.2, these expressions can be used to replace injected power terms in Eqs. (42) and (43) when written with separate sums over L_0, L_1 as in Eq. (23). Unlike Sect. 5.2, these expressions are also used to replace injected power terms in the power magnitude bounds Eq. (37) (written as two separate constraints, quantified over L_0 and L_1). This yields two fourth-degree polynomial inequality constraints in v which are linear in $\cos(\theta_b - \theta_a)$ and $\sin(\theta_b - \theta_a)$:

$$\begin{aligned}
&\forall (b,a,h) \in L_0 \ \left((Y^{\mathsf{ff}}_{bah})^{\mathsf{c}}\right)^2 v_b^4 + 2(Y^{\mathsf{ff}}_{bah})^{\mathsf{c}}(Y^{\mathsf{ft}}_{bah})^{\mathsf{c}} v_b^3 v_a \cos(\theta_b - \theta_a) \\
&\quad - 2(Y^{\mathsf{ff}}_{bah})^{\mathsf{c}}(Y^{\mathsf{ft}}_{bah})^{\mathsf{r}} v_b^3 v_a \sin(\theta_b - \theta_a) + \left((Y^{\mathsf{ft}}_{bah})^{\mathsf{c}}\right)^2 v_b^2 v_a^2 \\
&\quad + 2(Y^{\mathsf{ft}}_{bah})^{\mathsf{c}}(Y^{\mathsf{ff}}_{bah})^{\mathsf{r}} v_b^3 v_a \sin(\theta_b - \theta_a) + \left((Y^{\mathsf{ff}}_{bah})^{\mathsf{r}}\right)^2 v_b^4 \\
&\quad + 2(Y^{\mathsf{ff}}_{bah})^{\mathsf{r}}(Y^{\mathsf{ft}}_{bah})^{\mathsf{r}} v_b^3 v_a \cos(\theta_b - \theta_a) + \left((Y^{\mathsf{ft}}_{bah})^{\mathsf{r}}\right)^2 v_b^2 v_a^2 \leq \bar{S}^2_{bah} \qquad (77) \\
&\forall (b,a,h) \in L_1 \ \left((Y^{\mathsf{tf}}_{abh})^{\mathsf{c}}\right)^2 v_b^2 v_a^2 + 2(Y^{\mathsf{tf}}_{abh})^{\mathsf{c}}(Y^{\mathsf{tt}}_{abh})^{\mathsf{c}} v_b^3 v_a \cos(\theta_b - \theta_a) \\
&\quad + 2(Y^{\mathsf{tf}}_{abh})^{\mathsf{c}}(Y^{\mathsf{tt}}_{abh})^{\mathsf{r}} v_b^3 v_a \sin(\theta_b - \theta_a) + \left((Y^{\mathsf{tt}}_{abh})^{\mathsf{c}}\right)^2 v_b^4 \\
&\quad - 2(Y^{\mathsf{tt}}_{abh})^{\mathsf{c}}(Y^{\mathsf{tf}}_{abh})^{\mathsf{r}} v_b^3 v_a \sin(\theta_b - \theta_a) + \left((Y^{\mathsf{tf}}_{abh})^{\mathsf{r}}\right)^2 v_b^2 v_a^2 \\
&\quad + 2(Y^{\mathsf{tf}}_{abh})^{\mathsf{r}}(Y^{\mathsf{tt}}_{abh})^{\mathsf{r}} v_b^3 v_a \cos(\theta_b - \theta_a) + \left((Y^{\mathsf{tt}}_{abh})^{\mathsf{r}}\right)^2 v_b^4 \leq \bar{S}^2_{bah}. \qquad (78)
\end{aligned}$$

We remark that the generated power variables $\mathscr{S}$ appear in Eqs. (42) and (43), which, after the replacements mentioned above, are also part of this formulation.

5.4 Jabr's relaxation

A conic relaxation (Jabr 2006) (also called Jabr's *radial relaxation*) can be obtained from the polar ACOPF formulation by replacing $v_b v_a \cos(\theta_b - \theta_a)$ by a new variable c_{ba}, and $v_b v_a \sin(\theta_b - \theta_a)$ by a new variable s_{ba}. More precisely, we define an index set $R = R_1 \cup R_2$, where:

$$\begin{aligned}
R_1 &= \{(b,b) \mid b \in B\} \\
R_2 &= \{(b,a) \mid (b,a,1) \in L\}.
\end{aligned}$$

Now for all $(b,a) \in R$ we define new variables c_{ba}, s_{ba}. Jabr's relaxation relies on $c, s, \mathscr{S}$ as decision variables.

If the following conditions

$$\forall (b,a) \in R \quad c_{ba} = v_b v_a \cos(\theta_b - \theta_a) \qquad (79)$$
$$\forall (b,a) \in R \quad s_{ba} = v_b v_a \sin(\theta_b - \theta_a) \qquad (80)$$

held, then the Jabr's relaxation would turn out to be exact. From Eqs. (79) and (80) we infer:

$$\forall (b,a,1) \in L_0 \quad c_{ba} = c_{ab} \qquad (81)$$
$$\forall (b,a,1) \in L_0 \quad s_{ba} = -s_{ab} \qquad (82)$$
$$\forall b \in B \quad s_{bb} = 0 \qquad (83)$$
$$\forall b \in B \quad c_{bb} = v_b^2 \qquad (84)$$
$$\forall (b,a,1) \in L_0 \quad c_{ba}^2 + s_{ba}^2 = v_b^2 v_a^2. \qquad (85)$$

While the latter do not imply relaxation exactness, they are nonetheless valid constraints. Some of them are nonconvex, however, and two of them [Eqs. (84) and (85)] also involve the voltage magnitude variables v, which are not necessarily part of the relaxation. We therefore use Eq. (84) to replace v in Eq. (85), and relax the equality of Eq. (85) to a convex conic inequality:

$$\forall (b, a, 1) \in L_0 \quad c_{ba}^2 + s_{ba}^2 \leq c_{bb}\, c_{aa}. \tag{86}$$

Moreover, by Eq. (84) we also have

$$\forall b \in B \quad c_{bb} \geq 0. \tag{87}$$

We construct Jabr's relaxation as follows: the objective function is as in Eq. (9), but we also assume it is convex quadratic. The power generation bounds Eqs. (35) and (36) are also part of the formulation. By Eq. (84), the voltage magnitude bounds are

$$\forall b \in B \quad \underline{V}_b \leq c_{bb} \leq \overline{V}_b. \tag{88}$$

By Eqs. (56)–(58), Eq. (87), and the fact that

$$\begin{aligned} \forall (b, a, 1) \in L_0 \quad V_b\, V_a^* &= v_b e^{i\theta_b}\, v_a e^{-i\theta_a} = v_b v_a e^{i(\theta_b - \theta_a)} \\ &= v_b v_a \cos(\theta_b - \theta_a) + i\, v_b v_a \sin(\theta_b - \theta_a) \\ &= c_{ba} + i s_{ba}, \end{aligned} \tag{89}$$

the phase difference bounds turn out to be:

$$\forall (b, a, h) \in L_0 \quad \tan(\underline{\eta}_{bah})\, c_{ba} \leq s_{ba} \leq \tan(\overline{\eta}_{bah})\, c_{ba} \tag{90}$$

$$\forall (b, a, h) \in L_0 \quad c_{ba} \geq 0. \tag{91}$$

We obtain expression for the injected power by replacement of Eqs. (79) and (80) in Eqs. (73)–(76):

$$\forall (b, a, h) \in L_0 :$$

$$(S_{bah})^{\mathsf{r}} = (Y_{bah}^{\mathsf{ff}})^{\mathsf{r}} c_{bb} + (Y_{bah}^{\mathsf{ft}})^{\mathsf{r}} c_{ba} + (Y_{bah}^{\mathsf{ft}})^{\mathsf{c}} s_{ba} \tag{92}$$

$$(S_{bah})^{\mathsf{c}} = -(Y_{bah}^{\mathsf{ff}})^{\mathsf{c}} c_{bb} + (Y_{bah}^{\mathsf{ft}})^{\mathsf{r}} s_{ba} - (Y_{bah}^{\mathsf{ft}})^{\mathsf{c}} c_{ba} \tag{93}$$

$$\forall (b, a, h) \in L_1 :$$

$$(S_{bah})^{\mathsf{r}} = (Y_{abh}^{\mathsf{tt}})^{\mathsf{r}} c_{bb} + (Y_{abh}^{\mathsf{tf}})^{\mathsf{r}} c_{ba} + (Y_{abh}^{\mathsf{tf}})^{\mathsf{c}} s_{ba} \tag{94}$$

$$(S_{bah})^{\mathsf{c}} = -(Y_{abh}^{\mathsf{tt}})^{\mathsf{c}} c_{bb} + (Y_{abh}^{\mathsf{tf}})^{\mathsf{r}} s_{ba} - (Y_{abh}^{\mathsf{tf}})^{\mathsf{c}} c_{ba}. \tag{95}$$

As in Sect. 5.2, these expressions can be used to replace injected power terms in Eqs. (42) and (43) when written with separate sums over L_0, L_1 as in Eq. (23). Concerning the injected power bound inequalities Eq. (37) (written as two separate constraints, quantified over L_0 and L_1), since Eqs. (92)–(95) are linear in c, s, we obtain the quadratic inequalities:

$$\begin{aligned}
\forall (b,a,h) \in L_0 \quad & \left((Y^{\mathrm{ff}}_{bah})^{\mathrm{c}}\right)^2 c^2_{bb} + 2\,(Y^{\mathrm{ff}}_{bah})^{\mathrm{c}}(Y^{\mathrm{ft}}_{bah})^{\mathrm{c}} c_{bb}c_{ba} \\
& - 2\,(Y^{\mathrm{ff}}_{bah})^{\mathrm{c}}(Y^{\mathrm{ft}}_{bah})^{\mathrm{r}} c_{bb}s_{ba} + \left((Y^{\mathrm{ff}}_{bah})^{\mathrm{r}}\right)^2 c^2_{bb} \\
& + 2\,(Y^{\mathrm{ff}}_{bah})^{\mathrm{r}}(Y^{\mathrm{ft}}_{bah})^{\mathrm{c}} c_{bb}s_{ba} + 2\,(Y^{\mathrm{ff}}_{bah})^{\mathrm{r}}(Y^{\mathrm{ft}}_{bah})^{\mathrm{r}} c_{bb}c_{ba} \\
& + \left((Y^{\mathrm{ft}}_{bah})^{\mathrm{c}}\right)^2 c_{bb}c_{aa} + \left((Y^{\mathrm{ft}}_{bah})^{\mathrm{r}}\right)^2 c_{bb}c_{aa} \le \bar{S}^2_{bah} \qquad (96) \\
\forall (b,a,h) \in L_1 \quad & \left((Y^{\mathrm{tf}}_{abh})^{\mathrm{c}}\right)^2 c_{bb}c_{aa} + 2\,(Y^{\mathrm{tf}}_{abh})^{\mathrm{c}}(Y^{\mathrm{tt}}_{abh})^{\mathrm{c}} c_{bb}c_{ba} \\
& + 2\,(Y^{\mathrm{tf}}_{abh})^{\mathrm{c}}(Y^{\mathrm{tt}}_{abh})^{\mathrm{r}} c_{bb}s_{ba} + \left((Y^{\mathrm{tf}}_{abh})^{\mathrm{r}}\right)^2 c_{bb}c_{aa} \\
& - 2\,(Y^{\mathrm{tf}}_{abh})^{\mathrm{r}}(Y^{\mathrm{tt}}_{abh})^{\mathrm{c}} c_{bb}s_{ba} + 2\,(Y^{\mathrm{tf}}_{abh})^{\mathrm{r}}(Y^{\mathrm{tt}}_{abh})^{\mathrm{r}} c_{bb}c_{ba} \\
& + \left((Y^{\mathrm{tt}}_{abh})^{\mathrm{c}}\right)^2 c^2_{bb} + \left((Y^{\mathrm{tt}}_{abh})^{\mathrm{r}}\right)^2 c^2_{bb} \le \bar{S}^2_{bah}. \qquad (97)
\end{aligned}$$

We remark that Eqs. (81) and (82) are also part of the relaxation, and that the generated power variables $\mathscr{S}$ appear in Eqs. (42) and (43) with the replacements mentioned in Sect. 5.3.

5.5 Mixed formulation

An exact QCQP formulation can be derived from Jabr's conic relaxation by adding relationships between c, s variables and rectangular $V^{\mathrm{r}}, V^{\mathrm{c}}$ voltage variables. More precisely, the mixed formulation optimizes Eq. (9) subject to power generation bounds Eqs. (35) and (36), voltage magnitude bounds Eqs. (87) and (88), phase difference bounds Eqs. (90) and (91), power flow equations obtained by replacement of Eqs. (92)–(95) into Eqs. (42)–(43) written as Eq. (23), power magnitude bounds Eqs. (96)–(97), symmetry relations Eqs. (81)–(82), as well as:

$$\begin{aligned}
\forall b \in B \quad & c_{bb} = (V_b{}^{\mathrm{r}})^2 + (V_b{}^{\mathrm{c}})^2 \qquad (98) \\
\forall (b,a,1) \in L_0 \quad & c_{ba} = V_b{}^{\mathrm{r}} V_a{}^{\mathrm{r}} + V_b{}^{\mathrm{c}} V_a{}^{\mathrm{c}} \qquad (99) \\
\forall (b,a,1) \in L_0 \quad & s_{ba} = V_b{}^{\mathrm{c}} V_a{}^{\mathrm{r}} - V_b{}^{\mathrm{r}} V_a{}^{\mathrm{c}}. \qquad (100)
\end{aligned}$$

The exactness of the mixed formulation follows from the exactness of the polar formulation in Sect. 5.3, the relations Eqs. (79)–(80), the fact Eq. (89), and the identities Eq. (55).

5.6 Matrix formulation

In this section, we show a matrix formulation of the voltage-only formulation presented above. This formulation is the one usually developed in solvers and it is inspired on the ones found in Lavaei and Low (2012) and Molzahn and Hiskens (2019).

Rearranging terms, from Eq. (26) we have that for each bus $b \in B$,

$$\sum_{g \in \mathscr{G}_b} \mathscr{S}_g - \tilde{S}_b = A_b^* |V_b|^2 + \sum_{(b,a,h) \in L_0} (\, Y^{\mathrm{ff}}_{bah}{}^* |V_b|^2 + Y^{\mathrm{ft}}_{bah}{}^* V_b\, V_a^*) +$$

$$+ \sum_{(b,a,h)\in L_1} (Y^{\mathsf{tf}}_{abh}{}^{*} V_b\, V_a^{*} + Y^{\mathsf{tt}}_{abh}{}^{*} |V_b|^2). \tag{101}$$

The left hand side (lhs) of Eq. (101) equals the net complex power injected to bus b. This equation can be rewritten as follows:

$$\sum_{g\in\mathscr{G}_b} \mathscr{S}_g - \tilde{S}_b = V_b \Bigg[A_b^{*} V_b^{*} + \sum_{(b,a,h)\in L_0} (Y^{\mathsf{ff}}_{bah}{}^{*} V_b^{*} + Y^{\mathsf{ft}}_{bah}{}^{*} V_a^{*}) + \\ + \sum_{(b,a,h)\in L_1} (Y^{\mathsf{tf}}_{abh}{}^{*} V_a^{*} + Y^{\mathsf{tt}}_{abh}{}^{*} V_b^{*}) \Bigg]. \tag{102}$$

In Sect. 3.2 we defined the admittance matrix $\mathbf{Y}_{ba}$ of the line (b, a). Now, we define the admitance matrix of the network, let $\mathcal{Y} \in \mathbb{C}^{n\times n}$ be defined by

$$\forall b \in B \quad \mathcal{Y}_{bb} = A_b + \sum_{(b,a,h)\in L_0} Y^{\mathsf{ff}}_{bah} + \sum_{(b,a,h)\in L_1} Y^{\mathsf{tt}}_{abh}$$
$$\forall b, a \in B, b \neq a \quad \mathcal{Y}_{ba} = \sum_{(b,a,h)\in L_0} Y^{\mathsf{ft}}_{bah} + \sum_{(b,a,h)\in L_1} Y^{\mathsf{tf}}_{abh}.$$

Denote by $e_1, \ldots, e_n$ the standard basis vectors in $\mathbb{R}^n$. Let $\Psi_b := e_b e_b{}^{\top} \mathcal{Y}$, define the voltage vector $V := (V_1 \ \cdots \ V_n)^{\top}$ and the matrix $W := \begin{bmatrix} V^{\mathsf{r}} \\ V^{\mathsf{c}} \end{bmatrix} \begin{bmatrix} V^{\mathsf{r}} \\ V^{\mathsf{c}} \end{bmatrix}^{\top}$. Therefore, Eq. (102) can be expressed as:

$$\begin{aligned}
\sum_{g\in\mathscr{G}_b} \mathscr{S}_g - \tilde{S}_b &= V_b \sum_{a\in B} \mathcal{Y}_{ba}{}^{*} V_a^{*} = V_b\, (e_b{}^{\top} \mathcal{Y} V)^{*} \\
&= (e_b{}^{\top} V)(V^{\mathsf{H}} \mathcal{Y}^{\mathsf{H}} e_b) = (V^{\mathsf{H}} \mathcal{Y}^{\mathsf{H}} e_b)(e_b{}^{\top} V) \\
&= (V^{\mathsf{H}} \Psi_b V)^{*} \\
&= \left((V^{\mathsf{r}} - iV^{\mathsf{c}})^{\top} (\Psi_b^{\mathsf{r}} + i\Psi_b^{\mathsf{c}})(V^{\mathsf{r}} + iV^{\mathsf{c}})\right)^{*} \\
&= (V^{\mathsf{r}\top} \Psi_b^{\mathsf{r}} V^{\mathsf{r}} + V^{\mathsf{c}\top} \Psi_b^{\mathsf{r}} V^{\mathsf{c}} + V^{\mathsf{c}\top} \Psi_b^{\mathsf{c}} V^{\mathsf{r}} - V^{\mathsf{r}\top} \Psi_b^{\mathsf{c}} V^{\mathsf{c}}) \\
&\quad + i(V^{\mathsf{c}\top} \Psi_b^{\mathsf{r}} V^{\mathsf{r}} - V^{\mathsf{r}\top} \Psi_b^{\mathsf{r}} V^{\mathsf{c}} - V^{\mathsf{r}\top} \Psi_b^{\mathsf{c}} V^{\mathsf{r}} - V^{\mathsf{c}\top} \Psi_b^{\mathsf{c}} V^{\mathsf{c}}) \\
&= \begin{bmatrix} V^{\mathsf{r}} \\ V^{\mathsf{c}} \end{bmatrix}^{\top} \begin{bmatrix} \Psi_b^{\mathsf{r}} & -\Psi_b^{\mathsf{c}} \\ \Psi_b^{\mathsf{c}} & \Psi_b^{\mathsf{r}} \end{bmatrix} \begin{bmatrix} V^{\mathsf{r}} \\ V^{\mathsf{c}} \end{bmatrix} - i \begin{bmatrix} V^{\mathsf{r}} \\ V^{\mathsf{c}} \end{bmatrix}^{\top} \begin{bmatrix} \Psi_b^{\mathsf{c}} & \Psi_b^{\mathsf{r}} \\ -\Psi_b^{\mathsf{r}} & \Psi_b^{\mathsf{c}} \end{bmatrix} \begin{bmatrix} V^{\mathsf{r}} \\ V^{\mathsf{c}} \end{bmatrix} \\
&= \frac{1}{2} \begin{bmatrix} V^{\mathsf{r}} \\ V^{\mathsf{c}} \end{bmatrix}^{\top} \begin{bmatrix} \Psi_b^{\mathsf{r}} + \Psi_b^{\mathsf{r}\top} & \Psi_b^{\mathsf{c}\top} - \Psi_b^{\mathsf{c}} \\ \Psi_b^{\mathsf{c}} - \Psi_b^{\mathsf{c}\top} & \Psi_b^{\mathsf{r}} + \Psi_b^{\mathsf{r}\top} \end{bmatrix} \begin{bmatrix} V^{\mathsf{r}} \\ V^{\mathsf{c}} \end{bmatrix} \\
&\quad - i \frac{1}{2} \begin{bmatrix} V^{\mathsf{r}} \\ V^{\mathsf{c}} \end{bmatrix}^{\top} \begin{bmatrix} \Psi_b^{\mathsf{c}} + \Psi_b^{\mathsf{c}\top} & \Psi_b^{\mathsf{r}} - \Psi_b^{\mathsf{r}\top} \\ \Psi_b^{\mathsf{r}\top} - \Psi_b^{\mathsf{r}} & \Psi_b^{\mathsf{c}} + \Psi_b^{\mathsf{c}\top} \end{bmatrix} \begin{bmatrix} V^{\mathsf{r}} \\ V^{\mathsf{c}} \end{bmatrix}.
\end{aligned} \tag{103}$$

In consequence, the power flow balance equations are:

$$\sum_{g\in\mathscr{G}_b} \mathscr{S}_g{}^{\mathsf{r}} - \tilde{S}_b^{\mathsf{r}} = \mathsf{Tr}\left(\frac{1}{2}\begin{bmatrix} \Psi_b^{\mathsf{r}} + \Psi_b^{\mathsf{r}\top} & \Psi_b^{\mathsf{c}\top} - \Psi_b^{\mathsf{c}} \\ \Psi_b^{\mathsf{c}} - \Psi_b^{\mathsf{c}\top} & \Psi_b^{\mathsf{r}} + \Psi_b^{\mathsf{r}\top} \end{bmatrix}\begin{bmatrix} V^{\mathsf{r}} \\ V^{\mathsf{c}} \end{bmatrix}\begin{bmatrix} V^{\mathsf{r}} \\ V^{\mathsf{c}} \end{bmatrix}^\top\right)$$
$$\sum_{g\in\mathscr{G}_b} \mathscr{S}_g{}^{\mathsf{c}} - \tilde{S}_b^{\mathsf{c}} = \mathsf{Tr}\left(\frac{-1}{2}\begin{bmatrix} \Psi_b^{\mathsf{c}} + \Psi_b^{\mathsf{c}\top} & \Psi_b^{\mathsf{r}} - \Psi_b^{\mathsf{r}\top} \\ \Psi_b^{\mathsf{r}\top} - \Psi_b^{\mathsf{r}} & \Psi_b^{\mathsf{c}} + \Psi_b^{\mathsf{c}\top} \end{bmatrix}\begin{bmatrix} V^{\mathsf{r}} \\ V^{\mathsf{c}} \end{bmatrix}\begin{bmatrix} V^{\mathsf{r}} \\ V^{\mathsf{c}} \end{bmatrix}^\top\right).$$

Finally, we write

$$\sum_{g\in\mathscr{G}_b} \mathscr{S}_g = \tilde{S}_b + \mathsf{Tr}(\mathbf{\Psi}_b W) + i\mathsf{Tr}(\hat{\mathbf{\Psi}}_b W) \tag{104}$$

where

$$\mathbf{\Psi}_b := \frac{1}{2}\begin{bmatrix} \Psi_b^{\mathsf{r}} + \Psi_b^{\mathsf{r}\top} & \Psi_b^{\mathsf{c}\top} - \Psi_b^{\mathsf{c}} \\ \Psi_b^{\mathsf{c}} - \Psi_b^{\mathsf{c}\top} & \Psi_b^{\mathsf{r}} + \Psi_b^{\mathsf{r}\top} \end{bmatrix}, \qquad \hat{\mathbf{\Psi}}_b := \frac{-1}{2}\begin{bmatrix} \Psi_b^{\mathsf{c}} + \Psi_b^{\mathsf{c}\top} & \Psi_b^{\mathsf{r}} - \Psi_b^{\mathsf{r}\top} \\ \Psi_b^{\mathsf{r}\top} - \Psi_b^{\mathsf{r}} & \Psi_b^{\mathsf{c}} + \Psi_b^{\mathsf{c}\top} \end{bmatrix}.$$

On the other hand, the flow on a branch $(b, a, h) \in L$ can be written as follows. Define

$$\Phi_{bah} := \begin{cases} Y_{bah}^{\mathsf{ff}} e_b e_b{}^\top + Y_{bah}^{\mathsf{ft}} e_b e_a{}^\top, & \text{if } (b,a,h) \in L_0 \\ Y_{abh}^{\mathsf{tf}} e_b e_a{}^\top + Y_{abh}^{\mathsf{tt}} e_b e_b{}^\top, & \text{if } (b,a,h) \in L_1. \end{cases}$$

Then,

$$S_{bah} = V^{\mathsf{H}} \Phi_{bah}{}^{\mathsf{H}} V = (V^{\mathsf{H}} \Phi_{bah} V)^*,$$

and, by following the steps in Eq. (103), we have

$$\begin{aligned} S_{bah} &= \mathsf{Tr}(\mathbf{\Phi}_{bah} W) + i\mathsf{Tr}(\hat{\mathbf{\Phi}}_{bah} W) \qquad (105)\\ \text{where} \quad \mathbf{\Phi}_{bah} &:= \frac{1}{2}\begin{bmatrix} \Phi_{bah}^{\mathsf{r}} + \Phi_{bah}^{\mathsf{r}\top} & \Phi_{bah}^{\mathsf{c}\top} - \Phi_{bah}^{\mathsf{c}} \\ \Phi_{bah}^{\mathsf{c}} - \Phi_{bah}^{\mathsf{c}\top} & \Phi_{bah}^{\mathsf{r}} + \Phi_{bah}^{\mathsf{r}\top} \end{bmatrix} \\ \text{and} \quad \hat{\mathbf{\Phi}}_{bah} &:= \frac{-1}{2}\begin{bmatrix} \Phi_{bah}^{\mathsf{c}} + \Phi_{bah}^{\mathsf{c}\top} & \Phi_{bah}^{\mathsf{r}} - \Phi_{bah}^{\mathsf{r}\top} \\ \Phi_{bah}^{\mathsf{r}\top} - \Phi_{bah}^{\mathsf{r}} & \Phi_{bah}^{\mathsf{c}} + \Phi_{bah}^{\mathsf{c}\top} \end{bmatrix}. \end{aligned}$$

Therefore, thanks to Shur's complement formula, the power flow constraint $|S_{bah}|^2 = \mathsf{Tr}(\mathbf{\Phi}_{bah} W)^2 + \mathsf{Tr}(\hat{\mathbf{\Phi}}_{bah} W)^2 \leq \bar{S}_{bah}^2$ can be written as the PSD constraint

$$\begin{bmatrix} -\bar{S}_{bah}^2 & \mathsf{Tr}(\mathbf{\Phi}_{bah} W) & \mathsf{Tr}(\hat{\mathbf{\Phi}}_{bah} W) \\ \mathsf{Tr}(\mathbf{\Phi}_{bah} W) & -1 & 0 \\ \mathsf{Tr}(\hat{\mathbf{\Phi}}_{bah} W) & 0 & -1 \end{bmatrix} \preceq 0. \tag{106}$$

Moreover, since $V_b\, V_a^* = (V^{\mathsf{H}} e_b e_a{}^{\top} V)^*$,

$$\begin{aligned} V_b\, V_a^* &= \mathsf{Tr}(\boldsymbol{\Theta}_{ba} W) + i\mathsf{Tr}(\hat{\boldsymbol{\Theta}}_{ba} W) \\ \text{where} \quad \boldsymbol{\Theta}_{ba} &:= \frac{1}{2}\begin{bmatrix} e_b e_a{}^{\top} + e_a e_b{}^{\top} & 0 \\ 0 & e_b e_a{}^{\top} + e_a e_b{}^{\top} \end{bmatrix} \\ \text{and} \quad \hat{\boldsymbol{\Theta}}_{ba} &:= \frac{-1}{2}\begin{bmatrix} 0 & e_b e_a{}^{\top} - e_a e_b{}^{\top} \\ e_a e_b{}^{\top} - e_b e_a{}^{\top} & 0 \end{bmatrix}. \end{aligned} \tag{107}$$

Using the representation of the balance equations, the power flow and the multiplication of voltages expressed in Eqs. (104), (105) and (107), we obtain the following formulation of the ACOPF problem presented in the previous sections, over the variables $V^{\mathsf{r}}, V^{\mathsf{c}} \in \mathbb{R}^n$, $W \in \mathbb{R}^{2n\times 2n}$ and $\mathscr{S}_g \in \mathbb{C}$ for each $g \in \mathscr{G}$:

$$\left.\begin{array}{rc} \min & \sum_{g\in\mathscr{G}} (c_{g1}\mathscr{S}_g{}^{\mathsf{r}} + c_{g0}) \\ \forall g \in \mathscr{G} & \underline{\mathscr{S}}_g \le \mathscr{S}_g \le \overline{\mathscr{S}}_g \\ \forall b \in B & \tilde{S}_b + \mathsf{Tr}(\boldsymbol{\Psi}_b W) + i\mathsf{Tr}(\hat{\boldsymbol{\Psi}}_b W) = \sum_{g\in\mathscr{G}_b} \mathscr{S}_g \\ \forall (b,a,h) \in L & \mathsf{Tr}(\boldsymbol{\Phi}_{bah} W)^2 + \mathsf{Tr}(\hat{\boldsymbol{\Phi}}_{bah} W)^2 \le \bar{S}_{bah}^2 \\ \forall (b,a,h) \in L_0 & [\tan(\underline{\eta}_{bah}), \tan(\overline{\eta}_{bah})]\mathsf{Tr}(\boldsymbol{\Theta}_{ba} W) \ni \mathsf{Tr}(\hat{\boldsymbol{\Theta}}_{ba} W) \\ \forall (b,a,h) \in L_0 & \mathsf{Tr}(\boldsymbol{\Theta}_{ba} W) \ge 0 \\ & e_r{}^{\top} V^{\mathsf{c}} = 0 \quad \wedge \quad e_r{}^{\top} V^{\mathsf{r}} \ge 0 \\ \forall b \in B & \underline{V}_b^2 \le \mathsf{Tr}(\boldsymbol{\Theta}_{bb} W) \le \overline{V}_b^2 \\ & \begin{bmatrix} V^{\mathsf{r}} \\ V^{\mathsf{c}} \end{bmatrix}\begin{bmatrix} V^{\mathsf{r}} \\ V^{\mathsf{c}} \end{bmatrix}^{\top} = W. \end{array}\right\} \tag{108}$$

The reference bus constraint $e_r{}^{\top} V^{\mathsf{c}} = 0$ can be expressed in terms of W as $\begin{bmatrix} 0 \\ e_r \end{bmatrix}^{\top} W \begin{bmatrix} 0 \\ e_r \end{bmatrix} = 0$. Note that if $(V^{\mathsf{r}}, V^{\mathsf{c}}, W)$ is a feasible point of Eq. (108), then $(-V^{\mathsf{r}}, -V^{\mathsf{c}}, W)$ is also feasible (with the exception of constraint $e_r{}^{\top} V^{\mathsf{r}} \ge 0$) with the same objective function value. Therefore, we can omit constraint $e_r{}^{\top} V^{\mathsf{r}} \ge 0$ and choose the corresponding solution that satisfy this inequality.

We obtain a real SDP relaxation of Eq. (108) by relaxing the constraint $W = \begin{bmatrix} V^{\mathsf{r}} \\ V^{\mathsf{c}} \end{bmatrix}\begin{bmatrix} V^{\mathsf{r}} \\ V^{\mathsf{c}} \end{bmatrix}^{\top}$ to $W \succeq_{\mathsf{H}} 0$ and, therefore, we can omit the voltage variables in the formulation:

$$
\left.
\begin{array}{rcl}
\min & \displaystyle\sum_{g\in\mathscr{G}} (c_{g1}\mathscr{S}_g{}^{\mathsf{r}} + c_{g0}) & \\
\forall g \in \mathscr{G} & \underline{\mathscr{S}}_g \le \mathscr{S}_g \le \overline{\mathscr{S}}_g & \\
\forall b \in B & \tilde{S}_b + \mathsf{Tr}(\boldsymbol{\Psi}_b W) + i\mathsf{Tr}(\hat{\boldsymbol{\Psi}}_b W) = \displaystyle\sum_{g\in\mathscr{G}_b} \mathscr{S}_g & \\
\forall (b,a,h) \in L & \begin{bmatrix} -\bar{S}^2_{bah} & \mathsf{Tr}(\boldsymbol{\Phi}_{bah} W) & \mathsf{Tr}(\hat{\boldsymbol{\Phi}}_{bah} W) \\ \mathsf{Tr}(\boldsymbol{\Phi}_{bah} W) & -1 & 0 \\ \mathsf{Tr}(\hat{\boldsymbol{\Phi}}_{bah} W) & 0 & -1 \end{bmatrix} \preceq 0 & \\
\forall (b,a,h) \in L_0 & [\tan(\underline{\eta}_{bah}), \tan(\overline{\eta}_{bah})]\mathsf{Tr}(\boldsymbol{\Theta}_{ba} W) \ni \mathsf{Tr}(\hat{\boldsymbol{\Theta}}_{ba} W) & \\
\forall (b,a,h) \in L_0 & \mathsf{Tr}(\boldsymbol{\Theta}_{ba} W) \ge 0 & \\
& \mathsf{Tr}\left(\begin{bmatrix} 0 \\ e_r \end{bmatrix} \begin{bmatrix} 0 \\ e_r \end{bmatrix}^{\top} W \right) = 0 & \\
\forall b \in B & \underline{V}_b^2 \le \mathsf{Tr}(\boldsymbol{\Theta}_{bb} W) \le \overline{V}_b^2 & \\
& W \succeq_{\mathsf{H}} 0. &
\end{array}
\right\} \quad (109)
$$

6 Literature review

In this section we give a literature review of the ACOPF and its relationship with MP. This review is short in most respects. However, given the nature of our relaxed formulations in the technical parts above, we decided survey relaxations in more details (Sect. 6.6).

6.1 Generalities

Early formulations of the (feasibility-only version of the) ACOPF date back to the mid-twentieth century. Power flow equations, in their complex formulation, were stated in Van Ness and Griffin (1961), and solved using an implementation of Newton's method. Later on, this implementation was improved in Tinney and Hart (1967) using sparse matrix techniques, which allowed the solution of the problem on larger networks.

A comprehensive discussion of the power flow equations is developed in Power Systems textbooks, such as Andersson (2008), Bergen Arthur and Vijay (2000), Glover et al. (2008) and Monticelli (1999). The parameters involved in these equations, including transformer, phasors and other branch elements, are discussed in detail in Monticelli (1999, Ch. 4); this allows the formulation of power flow equations in complex and polar coordinates. The books Bergen Arthur and Vijay (2000) and Glover et al. (2008)) are devoted to the physics behind the model, with technical details of power system operations.

6.2 MP formulations

The optimization aspect of the problem was first introduced as "Economic Dispatch" in Carpentier (1962), followed by a survey of the state the art of the Optimal Power Flow (OPF) problem in DC in Carpentier (1979). Other extensive surveys (Huneault and Galiana 1991; Momoh et al. 1999a, b) of selected literature until the early nineties follow the evolution of the OPF and related solution methodologies. J.F. Bonnans published a series of three mathematically-oriented papers (Bonnans 1997, 1998, 2000) about OPF formulations: the second Bonnans (1998) concerns the feasibility and the third Bonnans (2000) the optimality of the ACOPF. The more recent surveys (Frank et al. 2012a, b) give an overview of existing MP formulations in qualitative terms, and focus on optimization methods (deterministic, non-deterministic, hybrid) for solving them.

Many algorithms relying on Interior Point Methods (IPM) have been developed in the last three decades. An IPM for nonlinear programming based on perturbing the Karush-Kuhn-Tucker optimality conditions of the Cartesian (also known as "rectangular") formulation was described in Wei et al. (1998). The authors in Capitanescu et al. (2007) and Torres and Quintana (1998) propose primal-dual IPM for nonlinear programs suited for the ACOPF problem, using as well the rectangular formulation. Whereas Rider et al. (2004) and Wang et al. (2007) develop step length control techniques on the polar OPF formulation. The techniques in Wang et al. (2007) were implemented in the open-source MATPOWER package (Zimmermann et al. 2010) for MATLAB.

The study of OPF solutions on tree networks (also known as "radial networks" in the OPF literature) has allowed the development of interesting techniques. For instance, the change of variables used in the Jabr's relaxation (see Sect. 5.4) was introduced in Gómez Expósito and Romero Ramos (1999), where a Newton's method is proposed to solve the OPF problem in tree networks. An efficient IPM for conic quadratic programming applied to power flow equations on tree networks was later introduced in Jabr (2006) and then extended to more general networks (Jabr 2007, 2008).

A new mixed-combinatorial solution method for tree networks without transformers, based on graph reduction and expansion operators on the tree graph, was proposed in Beck et al. (2018). The reduction step repeatedly contracts leaf nodes in the star of some vertex v in the tree to v itself. At the same time, it updates voltage bounds at v so that they are feasible w.r.t. the ACOPF constraints imposed at the leaves. Such reductions are carried out until the only vertex left is the tree root. The opposite operation re-expands the tree while keeping voltage values feasible. The whole process appears to be similar to the well-known Feasibility-Based Bounds Tightening algorithm (Messine 1997; Belotti et al. 2010) used in spatial Branch-and-Bound (Shectman and Sahinidis 1998; Belotti et al. 2009).

6.3 Grid security

The vulnerability of the power grid has been a major concern in the past decade, after the occurrence of serious cyber-physical attacks affecting large geographical zones

(Sridhar et al. 2012). The security of networks and the repercussions of line failures, such as cascades and consequential blackouts, are discussed in detail in Bienstock (2016). False data injection attacks (Chaojun et al. 2015; Liu and Li 2017) aim at studying the potential threat of a cyber attack consisting in modifying the voltage measurements of the grid, which would trick the network controller into taking wrong decisions. More complicated (but possible) attacks include a physical alteration of the grid, such as disconnecting some lines or disturbing the load and generation of a zone of the grid (Soltan and Zussman 2017; Bienstock and Escobar 2020).

These attacks rely on the ability that a network controller has to recover or estimate the status of the system—voltages, flows, generation and loads—from the measurement of a (reduced) subset of these physical quantities. Since the actions that the network controller subsequently takes depend on the estimation that he or she makes of the grid status, any possible error on this process can be crucial in order to maintain the system stability. A stochastic defense mechanism that randomly perturbs the power generation in order to unmask the effect of sophisticated attacks is proposed in Bienstock and Escobar (2020).

We note that many of these formulations employ binary or integer variables in order to model attacks or other vulnerabilities.

6.4 Optimal transmission switching

The Optimal Transmission Switching (OTS) problem (Fisher et al. 2008; Hedman et al. 2008) aims at optimizing the electrical network by controlling which transmission lines are going to be active during normal operation. Lines can be activated through circuit breakers, the status of which is controlled by corresponding decision variables in formulations. The model proposed in Fisher et al. (2008) is based on a DCOPF formulation, which yields a Mixed Integer Linear Program. The authors show improvements of 20% in the generation cost in the IEEE 118-bus test network achieved by allowing at most three lines to be open, an improvement of 25% is shown when there is no constraint on the number of lines that can be open.

Given the computational difficulty, most of the literature related to the OTS problem has been focused on the DCOPF formulation, which is not in the scope of this survey. However, some OTS works are indeed based on the ACOPF (Khanabadi et al. 2013; Barrows et al. 2014; Bienstock and Muñoz 2015; Henneaux and Kirschen 2016; Hijazi et al. 2017; Lan et al. 2018; Lu et al. 2018; Zhao et al. 2019; Bélanger et al. 2020; Brown and Moreno-Centeno 2020). In particular, Khanabadi and Ghasemi (2011) proposes an iterative scheme with the DC OTS problem and a subsequent verification of the ACOPF feasibility considering the new topology. If the ACOPF does not find an acceptable solution, the lines that the OTS proposed to open are removed from the set of switching branches and the iteration continues; Potluri and Hedman (2012) solves the ACOPF on the IEEE 118-bus case by removing one branch at a time. Moreover, the authors numerically show that an improvement on generation obtained by opening a line in the DCOPF results in a greater generation cost in the ACOPF, and *vice versa*. A new exact formulation for AC OTS and a mixed-integer second-order cone programming relaxation is proposed in Kocuk et al. (2017), along with a heuristic

designed to obtain high quality feasible solutions; the relaxation is improved by strong valid inequalities for AC OPF inspired by Kocuk et al. (2016).

Additional ACOPF-based heuristics for the OTS problem have been proposed in Potluri and Hedman (2012), Soroush and Fuller (2014) and Capitanescu and Wehenkel (2014).

6.5 Network design

Another family of ACOPF formulation variants that depend on binary variables, related to those in Sect. 6.4, are the formulations derived from network design. To the best of our knowledge, the first paper exhibiting computational results for the ACOPF with binary variables used for design purposes is Ruiz et al. (2014), where binary variables are used to switch generators and shunts on and off. Improved formulations with binary variables for switching generators on and off were proposed in Salgado et al. (2018b, a). The ACOPF is **NP**-hard (Bienstock and Verma 2019), and remains hard even when the goal is to minimize the number of active generators (Salgado et al. 2018a).

6.6 Relaxations

SDP relaxations based on the ACOPF formulation in rectangular coordinates have also been studied. Sufficient conditions are exhibited in Lavaei and Low (2012) for ACOPF instances to have zero optimality gap with respect to their SDP relaxations. Moreover, optimal solutions of the original problem can be obtained from solutions of the SDP relaxation. However, Lesieutre et al. (2011) proves that this SDP relaxation is not exact for a specific example of a cycle of three buses and, consequently, that it would fail on larger networks including cycles. A relaxation of the ACOPF, based on Lasserre's moments hierarchy (Putinar 2011) applied to the rectangular V-formulation, is shown in Molzahn and Hiskens (2014, 2015) to improve results obtained by previous relaxations, such as Lavaei and Low (2012).

An extensive survey of convex formulations of the ACOPF can be found in Low (2013, 2014a, b). Moreover, Coffrin et al. (2016) compares—theoretically and numerically—quadratic convex relaxations derived from the complex formulation of the ACOPF problem with SDP and second order cone relaxations. A Second-Order Cone Programming (SOCP) relaxation in the 2×2 minors of the Hermitian matrix variable representing voltage in rectangular coordinates is proposed in Kocuk et al. (2018), and compared with state-of-the-art SDP relaxations.

6.6.1 Zero duality gaps in SDP relaxations

The authors of Lavaei and Low (2012) consider the dual of a real SDP relaxation of the ACOPF. Under particular conditions, the duality gap between primal and dual formulations is shown to be zero. A solution of the original OPF problem can therefore be recovered from the dual optimal solution. The dual SDP considered in Lavaei and Low (2012) is similar to Eq. (109). Table 1 shows the notational differences between

Table 1 Equivalence of notations between Eq. (109), Lavaei and Low (2012) and Molzahn et al. (2013)

Our notation	Notation in Lavaei and Low (2012)	Notation in Molzahn et al. (2013)	Comments
b	k	i	Generic bus
(b,a,h)	(l,m)	$k=(k_l,k_m)$	Generic line
V	$\mathbf{V}$		Vector of complex voltages
W	W	$\mathbf{W}$	
$\sum_{g\in\mathcal{G}_b} \mathcal{S}_g$	$P_{G_k}+iQ_{G_k}$	$\sum_{g\in\mathcal{G}_i}(P_{G_g}+iQ_{G_g})$	Generation at a generic bus
$\tilde{S}_b$	$P_{D_k}+iQ_{D_k}$	$P_{D_i}+iQ_{D_i}$	Load at a generic bus
$\mathcal{Y}$	Y	$\mathbf{Y}$	Admittance matrix
Ψ_b	Y_k	Y_i	$\Psi_b=e_b e_b^\top \mathcal{Y}$
Constraint matrices			Related constraint
$\mathbf{\Psi}_b$	$\mathbf{Y}_k$	$\mathbf{Y}_i$	Real power injection
$\hat{\mathbf{\Psi}}_b$	$\bar{\mathbf{Y}}_k$	$\bar{\mathbf{Y}}_i$	Complex power injection
$\mathbf{\Theta}_{bb}$	M_k	$\mathbf{M}_i$	Voltage magnitude
$\mathbf{\Phi}_{bah}$	$\mathbf{Y}_{lm}$	$\begin{cases}\mathbf{Z}_{k_l}, & (b,a,h)\in L_0\\ \mathbf{Z}_{k_m}, & (b,a,h)\in L_1\end{cases}$	Branch active power flow
$\hat{\mathbf{\Phi}}_{bah}$	$\bar{\mathbf{Y}}_{lm}$	$\begin{cases}\bar{\mathbf{Z}}_{k_l}, & (b,a,h)\in L_0\\ \bar{\mathbf{Z}}_{k_m}, & (b,a,h)\in L_1\end{cases}$	Branch reactive power flow

Lavaei and Low (2012) and Eq. (109). There are four differences between these two formulations: (i) parallel lines are not considered in Lavaei and Low (2012); (ii) at most one generator is assumed to be attached to each bus in Lavaei and Low (2012), which allows the power balance equations to be replaced in the generated power bound inequalities; (iii) the power magnitude bound on lines in Lavaei and Low (2012) is only imposed on the real part of the power variables, i.e. $|S^{\mathrm{r}}_{bah}| \leq \overline{P}_{bah}$; (iv) the phase difference constraints are replaced by $|V_b - V_a| \leq \Delta_{ba}$, where Δ_{ba} is a given parameter.

The algorithm proposed in Lavaei and Low (2012) to obtain an optimal solution of the ACOPF is based on the zero duality gap between the ACOPF and the dual SDP relaxation: this occurs if the matrix

$$\begin{aligned} A(x,r) := \sum_{b\in B}(x_{b,1}\mathbf{\Psi}_b + x_{b,2}\hat{\mathbf{\Psi}}_b + x_{b,3}\mathbf{\Theta}_{bb}) + \\ + \sum_{(b,a,h)\in L}\big((2r_{bah,1}+x_{bah,1})\mathbf{\Phi}_{bah} + 2r_{bah,2}\hat{\mathbf{\Phi}}_{bah} + \\ + x_{bah,2}(\mathbf{\Theta}_{bb}+\mathbf{\Theta}_{aa}-2\mathbf{\Theta}_{ba})\big) \end{aligned}$$

found in the dual constraint $A(x,r) \succeq_{\mathsf{H}} 0$ (where $x \geq 0$ and r are the Lagrange multipliers associated to the primal constraints) has a zero eigenvalue of multiplicity at

most 2, when the matrix is evaluated in the dual optimal solution $(x^{\text{opt}}, r^{\text{opt}})$. Therefore, a globally optimal solution of the ACOPF can be recovered in polynomial time from a nonzero vector in the null space of the aforementioned matrix.

Similar conditions for ensuring zero duality gap for DC power distribution networks are also given in Lavaei and Low (2012). Moreover, it is shown that such conditions happen almost always in DC networks. Empirical results are shown to prove the efficiency of this method on IEEE benchmark systems with 14, 30, 57, 118, and 300 buses.

6.6.2 Applicability to real-life cases

The applicability of the ideas given in Lavaei and Low (2012) to real-life cases was carried out in a sequence of papers co-authored by Molzahn et al.

The generalizations put forth in Molzahn et al. (2014) are as follows: (i) non-zero line resistances are allows; (ii) conditions for zero duality gap are derived from the KKT conditions: given a solution V of the dual SDP relaxation in terms of voltage values, the corresponding rank one matrix W, and a dual feasible matrix $A \succeq_{\mathsf{H}} 0$, the value of the dual SDP relaxation is globally optimal for the ACOPF if A, W satisfy the slack complementarity condition $\mathsf{Tr}(AW) = 0$.

In Molzahn et al. (2013), the SDP formulations of Lavaei and Low (2012) are extended to the case of more than one generator connected to each bus, and multiple (parallel) lines between buses. Moreover, the generation cost may be a quadratic or piece-wise linear function of the real power generated. However, phase difference and reference voltage fixing constraints are not considered. The dual SDP relaxation presented in Molzahn et al. (2013) integrates these generalizations. An extension of the PSD matrix completion theorem in Jabr (2012) allows the replacement of the PSD variable matrix W (as mentioned above) by multiple but smaller-sized PSD variable matrices, at the cost of some additional linking constraints between the components of the smaller matrices. The size reduction extent depends on the sparsity of the power network G. The solution algorithm proposed in Molzahn et al. (2013) takes care of the trade-off between size reduction and the additional linking constraints. Numerical results show the efficiency of this method in large networks, such as the IEEE 300-bus system and the 3012-bus model of the Polish system.

We note that Table 1 also shows the notational differences with Molzahn et al. (2013). To help with readability, we also note that Molzahn et al. (2013, Prob. (2)) and Molzahn et al. (Molzahn et al. 2014, Prob. (10)) use the symbols S_k, S_{lm} to mean injected power on a line.

6.6.3 Use of Lasserre's relaxation hierarchies

As mentioned in Sect. 4.4, and in particular in Eq. (31), the ACOPF can be formulated as a QCQP, which is a Polynomial Programming (PP) problem of degree 2. Such formulations were investigated in Ghaddar et al. (2016) and Kuang et al. (2016). We report the formulation of interest using the notation introduced in Sect. 5.6, with

variables $\mathscr{S}_g^{\mathsf{r}}$, $S_{bah}{}^{\mathsf{r}}$, $S_{bah}{}^{\mathsf{c}}$ and $x = \left[V^{\mathsf{r}\top}\ V^{\mathsf{c}\top}\right]$:

$$\left.\begin{array}{rr}
\min & \sum_{g\in\mathscr{G}} (c_{g2}(\mathscr{S}_g^{\mathsf{r}})^2 + c_{g1}(\mathsf{Tr}(\boldsymbol{\Psi}_g xx^\top) + \tilde{S}_g^{\mathsf{r}}) + c_{g0}) \\
\forall b \in B & \underline{\mathscr{S}}_b{}^{\mathsf{r}} \le \mathsf{Tr}(\boldsymbol{\Psi}_b xx^\top) + \tilde{S}_b^{\mathsf{r}} \le \overline{\mathscr{S}}_b{}^{\mathsf{r}} \\
\forall b \in B & \underline{\mathscr{S}}_b{}^{\mathsf{c}} \le \mathsf{Tr}(\hat{\boldsymbol{\Psi}}_b xx^\top) + \tilde{S}_b^{\mathsf{c}} \le \overline{\mathscr{S}}_b{}^{\mathsf{c}} \\
\forall b \in B & \underline{V}_b^2 \le \mathsf{Tr}(\boldsymbol{\Theta}_{bb} xx^\top) \le \overline{V}_b^2 \\
\forall (b,a,h) \in L & (S_{bah}{}^{\mathsf{r}})^2 + (S_{bah}{}^{\mathsf{c}})^2 \le \tilde{S}_{bah}^2 \\
\forall g \in \mathscr{G} & \mathsf{Tr}(\boldsymbol{\Psi}_g xx^\top) + \tilde{S}_g^{\mathsf{r}} = \mathscr{S}_g{}^{\mathsf{r}} \\
\forall (b,a,h) \in L & \mathsf{Tr}(\boldsymbol{\Phi}_{bah} xx^\top) = S_{bah}{}^{\mathsf{r}} \\
\forall (b,a,h) \in L & \mathsf{Tr}(\hat{\boldsymbol{\Phi}}_{bah} xx^\top) = S_{bah}{}^{\mathsf{c}}.
\end{array}\right\} \tag{110}$$

We note that Ghaddar et al. (2016) and Kuang et al. (2016) assume that there are no parallel arcs, and that there is at most one generator attached to each bus. Moreover, the power flow equations are implicit in the power generation bounds, through the replacement $\underline{\mathscr{S}}_b = \sum_{g\in\mathscr{G}_b} \underline{\mathscr{S}}_g$ and $\overline{\mathscr{S}}_b = \sum_{g\in\mathscr{G}_b} \overline{\mathscr{S}}_g$, where the sums are equal to zero if $\mathscr{G}_b = \varnothing$.

The solution approaches in Ghaddar et al. (2016) and Kuang et al. (2016) are both based on the well-known Lasserre relaxation hierarchies (Lasserre 2009), which builds a sequence of SDP relaxations that approximate the dual of a PP such as Eq. (110). The decision variables of these SDP relaxations are the coefficients of the monomials appearing in Sum-Of-Squares (SOS) polynomials up to certain degree. A sequence of SDP relaxations is obtained by increasing the degree of the SOS polynomials, which in turn increases the tightness of the approximation.

The first level of the Lasserre hierarchy that approximates Eq. (110) is shown by Ghaddar et al. (2016) to be equivalent to the dual SDP relaxation in Lavaei and Low (2012) mentioned above. Linear and SOCP approximations of the SDP cone based on Diagonal Dominance (DD) were employed in Kuang et al. (2016) for more efficient computation, as explained in Ahmadi and Majumdar (2014, 2019).

The sparse structure of the polynomials involved in Eq. (110) is exploited in Kuang et al. (2016) in order to reduce the number of monomials appearing in the DD approximations of Lasserre's hierarchy (each approximating formulation in this hierarchy is called a "structured PP-SDSOS$_r$"). We note that this structure is also studied in Bose et al. (2015). The first level of the SOCP DD approximation of Lasserre's hierarchy is shown in Kuang et al. (2016) to be equivalent to the dual of the SOCP relaxation of the ACOPF presented in Bose et al. (2015):

$$\left.\begin{array}{cc}
\min & c(X) \\
\forall b \in B & \underline{\mathscr{S}}_b \le \sum_{a\in B} X_{ba}\, \mathcal{Y}_{ba}{}^* \le \overline{\mathscr{S}}_b \\
\forall b \in B & \underline{V}_b^2 \le X_{bb} \le \overline{V}_b^2 \\
\forall (b,a,1) \in L & X_{bb}X_{aa} \ge |X_{ba}|^2 \\
& X \in \mathbb{C}^{n\times n} \text{ hermitian},
\end{array}\right\} \tag{111}$$

where the variable X represent the terms found in the matrix VV^{H} (see first equality in Eq. (103), also see Sect. 4.4), $c(X)$ is one the typical cost function and the constraint

$X_{bb}X_{aa} \geq |X_{ba}|^2$ replaces the constraint that requires that the submatrix $\begin{bmatrix} X_{bb} & X_{ba} \\ X_{ab} & X_{aa} \end{bmatrix}$ is PSD (see Remark 1 in Bose et al. (2015) in regards to dealing with additional constraints, such as, bounds on power flows). The numerical results presented in Kuang et al. (2016) show the equivalence between the different problems stated above as well as trade-off between the time reduction resulting from the use of DD approximations and their precision.

6.6.4 Improving the optimality gap of SDP relaxations

Some interesting improvements to optimality gap given by SDP relaxations and the corresponding exact formulations are proposed in Gopinath et al. (2020). The SDP relaxation is approximated by a sequence of formulations, called the "determinant hierarchy", introduced in Hijazi et al. (2016). These approximations are applied to each level of Lasserre's hierarchy. Instead of requiring $U \succeq_{\mathsf{H}} 0$ for a given matrix in the SDP relaxation, the level k of the determinant hierarchy imposes that all square sub-matrices of U of size $\leq k$ should have non-negative determinant, which yields polynomial constraints of degree k.

It is shown in Madani et al. (2016) and Hijazi et al. (2016) that the higher level of the determinant hierarchy (the level equal to the size of the matrix dimension) applied to the complex SDP relaxation Eq. (34) corresponds to the replacement of constraint $X \succeq_{\mathsf{H}} 0$ by the constraints

$$\forall \mathcal{S} \subseteq \mathcal{C} \in \mathcal{T}(G) \qquad \det(X_{\mathcal{S}}) \geq 0, \tag{112}$$

where $\mathcal{T}(G)$ is a tree-decomposition (Diestel 2017) of the network G, $\mathcal{C}$ is one of the nodes of this tree-decomposition (which corresponds to a clique of G, thus, $\mathcal{C} \subseteq B$), and $\mathcal{S}$ is a sub-clique of $\mathcal{C}$. The matrix $X_{\mathcal{S}}$ is the submatrix of X resulting from restricting X to the columns and rows of X corresponding to the buses in $\mathcal{S}$. Since real-life networks are usually sparse, it is possible to describe them with a tree-decomposition where the cliques have small size and, therefore, the number of sub-cliques is polynomial on the size of B.

SDP relaxations and Reformulation-Linearization Technique (RLT) (Sherali and Alameddine 1992) cuts were shown to be complementary in Anstreicher (2009). This idea is applied to current and power expressions in Gopinath et al. (2020). Specifically, if Eqs. (19), (20) and (22) are multiplied by their conjugate, we obtain the constraints

$$\begin{aligned}
\forall (b,a,h) \in L \qquad & S_{bah}\, S_{bah}^* = V_b\, V_b^* I_{bah}\, I_{bah}^* \\
\forall (b,a,h) \in L_0 \qquad & I_{bah}\, I_{bah}^* = |Y_{bah}^{\mathsf{ff}}|^2 V_b\, V_b^* + Y_{bah}^{\mathsf{ff}}\, Y_{bah}^{\mathsf{ft}\,*} V_b\, V_a^* \\
& \qquad + Y_{bah}^{\mathsf{ft}}\, Y_{bah}^{\mathsf{ff}\,*} V_a\, V_b^* + |Y_{bah}^{\mathsf{ft}}|^2 V_a\, V_a^* \\
\forall (b,a,h) \in L_1 \qquad & I_{bah}\, I_{bah}^* = |Y_{abh}^{\mathsf{tf}}|^2 V_a\, V_a^* + Y_{abh}^{\mathsf{tf}}\, Y_{abh}^{\mathsf{tt}\,*} V_a\, V_b^* \\
& \qquad + Y_{abh}^{\mathsf{tt}}\, Y_{abh}^{\mathsf{tf}\,*} V_b\, V_a^* + |Y_{abh}^{\mathsf{tt}}|^2 V_b\, V_b^*,
\end{aligned}$$

which are then lifted to linear constraints using X and the new variables $\widehat{S_{bah}{}^{\mathsf{r}}}$, $\widehat{S_{bah}{}^{\mathsf{c}}}$, $\widehat{I_{bah}}$ and $\widehat{WI_{bah}}$ to represent the terms $(S_{bah}{}^{\mathsf{r}})^2$, $(S_{bah}{}^{\mathsf{c}})^2$, $|I_{bah}|^2$ and $W_{bb}\widehat{I_{bah}}$, respec-

tively:

$$\forall (b,a,h) \in L \quad \widehat{S_{bah}{}^{\mathsf{r}}} + \widehat{S_{bah}{}^{\mathsf{c}}} = \widehat{WI_{bah}} \tag{113}$$

$$\forall (b,a,h) \in L_0 \quad \widehat{I_{bah}} = |Y^{\mathsf{ff}}_{bah}|^2 X_{bb} + Y^{\mathsf{ff}}_{bah} \, Y^{\mathsf{ft}}_{bah}{}^{*} X_{ba} + Y^{\mathsf{ft}}_{bah} \, Y^{\mathsf{ff}}_{bah}{}^{*} X_{ab} + |Y^{\mathsf{ft}}_{bah}|^2 X_{aa} \tag{114}$$

$$\forall (b,a,h) \in L_1 \quad \widehat{I_{bah}} = |Y^{\mathsf{tf}}_{abh}|^2 X_{aa} + Y^{\mathsf{tf}}_{abh} \, Y^{\mathsf{tt}}_{abh}{}^{*} X_{ab} + Y^{\mathsf{tt}}_{abh} \, Y^{\mathsf{tf}}_{abh}{}^{*} X_{ba} + |Y^{\mathsf{tt}}_{abh}|^2 X_{bb}. \tag{115}$$

More precisely, a different convex relaxation is obtained from Eq. (34) with the following changes:

1. Equation (112) instead of constraint $X \succeq_{\mathsf{H}} 0$,
2. $\widehat{S_{bah}{}^{\mathsf{r}}} + \widehat{S_{bah}{}^{\mathsf{c}}} \leq \overline{S}^2_{bah}$ as apparent flow limit at every arc $(b,a,h) \in L$,
3. inclusion of Eqs. (113)–(115) for each arc $(b,a,h) \in L$,
4. $0 \leq \widehat{I_{bah}} \leq \overline{I}^2_{bah}$ as bounds for the squared current magnitude at each arc $(b,a,h) \in L$ [if the bound is not given, one could define $\overline{I}_{bah} := \overline{S}_{bah}/\underline{V}_b$, see Eqs. (27)–(30)],
5. McCormick convex envelopes (McCormick 1976) for the lifted variable $\widehat{WI_{bah}}$ of the bilinear term $W_{bb}\widehat{I_{bah}}$:

$$\begin{aligned}
&\forall (b,a,h) \in L \quad \underline{V}^2_b \widehat{I_{bah}} \leq \widehat{WI_{bah}} \leq \overline{V}^2_b \widehat{I_{bah}} \\
&\forall (b,a,h) \in L \quad \widehat{WI_{bah}} \geq \overline{V}^2_b \widehat{I_{bah}} + W_{bb}\overline{I}^2_{bah} - \overline{V}^2_b \overline{I}^2_{bah} \\
&\forall (b,a,h) \in L \quad \widehat{WI_{bah}} \leq W_{bb}\overline{I}^2_{bah} + \underline{V}^2_b \widehat{I_{bah}} - \underline{V}^2_b \overline{I}^2_{bah},
\end{aligned}$$

6. convexification of equations $\widehat{S_{bah}{}^{\mathsf{r}}} = (S_{bah}{}^{\mathsf{r}})^2$ and $\widehat{S_{bah}{}^{\mathsf{c}}} = (S_{bah}{}^{\mathsf{c}})^2$ defined by the inequalities:

$$\begin{aligned}
&\forall (b,a,h) \in L \quad (S_{bah}{}^{\mathsf{r}})^2 \leq \widehat{S_{bah}{}^{\mathsf{r}}} \leq S_{bah}{}^{\mathsf{r}}(\underline{P}_{bah} + \overline{P}_{bah}) - \underline{P}_{bah}\overline{P}_{bah} \\
&\forall (b,a,h) \in L \quad (S_{bah}{}^{\mathsf{c}})^2 \leq \widehat{S_{bah}{}^{\mathsf{c}}} \leq S_{bah}{}^{\mathsf{c}}(\underline{Q}_{bah} + \overline{Q}_{bah}) - \underline{Q}_{bah}\overline{Q}_{bah},
\end{aligned}$$

   where $\underline{P}_{bah}, \overline{P}_{bah}, \underline{Q}_{bah}, \overline{Q}_{bah}$ are lower/upper bounds for active and reactive power flows, one could take $-\underline{P}_{bah} = -\underline{Q}_{bah} = \overline{P}_{bah} = \overline{Q}_{bah} = \overline{S}_{bah}$.

It turns out that this convex relaxation may be less tight w.r.t. Eq. (34), but it can also be solved more efficiently, and hence larger instances can be tackled. See Coffrin et al. (2017) for more details.

An algorithm called SDP-based Bound Tightening based on Optimimality-based Bound Tightening (Zamora and Grossmann 1999; Gleixner et al. 2017) is proposed in Gopinath et al. (2020). This algorithm alternately solves two types of sub-problems: (i) the convex ACOPF relaxation described above and (ii) a problem that minimizes (maximizes) one of the variables of this convex relaxation, subject to the original cost function bounded by the cost of a feasible solution, to find a tighter lower (upper)

bound for the variable. The algorithm iterates between problem (i) and a set of problems of type (ii) obtained by considering different variables and whether it minimizes or maximizes the selected variable, the authors remark this second stage of the iterations can be parallelized through the consideration of the different sub-problems of type (ii).

The approach proposed in Gopinath et al. (2020) is supported by numerical experiments on cases from benchmark libraries Babaeinejadsarookolaee (2019, v19.05) and Coffrin et al. (2014, v0.3). These experiments compare the gap obtained at the end of the algorithm with the gap of the two first levels of Lasserre's hierarchy. In the first library, the optimality gap obtained from the algorithm was less that 1% on all tested instances (networks with 300 buses or less).

7 Conclusion

In this technical survey, we reviewed the alternating current optimal power flow problem and its modelling by mathematical programming. We presented continuous variable formulations in complex and real numbers, involving both polynomial and trigonometric terms, as well as relaxations based on several techniques, e.g. semidefinite and second-order cone programming. Most of the formulations discussed in this survey have been modelled and tested on a few instances to verify consistency and reduce the occurrences of typos and errors (see the "Appendices" below).

There are currently multiple challenges in this field. A notable one is to bridge the technical language of the power engineering community (both industrial and academic) to other complementary fields of knowledge: this survey is intended as a contribution in this sense. We hope it will serve as a technical key to help operations researchers understand the details of power flow formulations in alternating current. The second challenge is to solve instances of this problem at national levels, i.e. of very large size, to global optimality in relatively short times; there is a widespread belief (for obvious reasons) that the answer will come from relaxations, which is why we reviewed the latest contributions in Sect. 6.6—some researchers, however, also think that good, special-purpose, fast solvers deployed on the original problem are essential to this purpose (Gilbert and Josz 2017). The third challenge, which we barely touched on, is to use the formulations presented above as a basis for more complicated formulations addressing security, design, distribution integration, and whole supply chain issues: we believe that such derived applications should be of interest to the operations research community at large.

Acknowledgements We are grateful to Cedric Josz and to Kundan Guha for interesting technical discussions.

Compliance with ethical standards

Conflict of interest The authors declare that they have no conflict of interest.

Appendix A: Computational consistency check

Many of the formulations discussed in this survey have been tested computationally. These tests were not designed to establish whether a formulation can be solved faster, or whether a relaxation is tighter, than another. The sheer complication of these formulations can be a formidable hurdle to their successful deployment, and previous experience from all of the authors confirmed that it is extremely difficult to remove all of the bugs. We therefore employed computational tests as a validity and consistency check.

A.1 Modelling platforms

We used three modelling platforms for implementing our formulations.

1. AMPL (Fourer and Gay 2002) is a commercial, command-line interpreter which offers an incomparably elegant language, yielding code which is very similar to the formulations as they are presented mathematically on the written page. Its expression terms, objectives, and constraints may be quantified by indices varying on a set. AMPL has two serious limitations: (a) the amount of post-processing which can be expressed by its imperative sublanguage is limited (e.g. there is no function for computing eigenvalues/eigenvectors or the inverse of a matrix); (b) there is no interface with most SDP solvers.
2. Python (van Rossum et al. 2019) is a *de facto* standard in "scripting programming". It is an interpreted language, with relatively low interpretation overhead CPU costs, and with a considerably large set of external modules (both interpreted and compiled), which allow the user to rapidly code almost anything. An equally large corpus of online documentation makes it possible to solve and issues using a simple internet query. We used the `cvxpy` (Diamond and Boyd 2016) MP modelling interface, which allows the coding and solution of SDPs and SOCPs using a range of solvers.
3. MATLAB (2017) is a well-known commercial "general-purpose" applied mathematical software package. It offers very good MP capabilities through a range of interfaces. We used YALMIP (Löfberg 2004), which, notably, also connects to SDP solvers.

Specifically, we implemented and tested:

- the real cartesian (S, I, V)-formulation (Sect. 5.1), the real cartesian voltage-only QCQP formulation (Sect. 5.2), the real polar NLP formulation (also in Sect. 5.2), and Jabr's (real) relaxation (Sect. 5.4) using AMPL;
- the complex SDP relaxation Eq. (33) (Sect. 4.4) using `cvxpy` on Python3;
- the real matrix formulation (Sect. 5.6) using YALMIP on MATLAB.

A.2 Solvers

We solved our formulations with a variety of solvers, some global and some local (used within a multi-start heuristic): Baron (Sahinidis and Tawarmalani 2005), Couenne

(Belotti et al. 2009), ECOS (Domahidi et al. 2013), Mosek (Mosek 2016), IPOpt (COIN-OR 2006), Snopt (Gill 1999). We remark that Baron cannot deal with trigonometric functions. We found that `cvxpy` was able to pass complex number SDPs to ECOS correctly, but not (always) to Mosek. The global solvers for NLP (Baron, Couenne), could never certify global optima, even for the smallest instances, testifying to the practical hardness of the ACOPF.

On the other hand, Baron's "upper bounding heuristic", consisting in a multi-start on various local NLP solvers, yielded best solutions. Our benchmark was formed by small instances in MATLAB's MATPOWER's (Zimmermann and Murillo-Sánchez 2018) `data` folder, and our comparison stone by the optima found by MATPOWER's own local NLP solver—a MATLAB implementation of a standard interior point method algorithm—from the local optima stored in the instances.

A.3 Notes

We also implemented a symbolic computation code [provided by `sympy` (Meurer et al. 2017)] in order to derive the the real expressions of formulations in real numbers from the corresponding complex expressions occurring in their complex counterparts.

Most of the code we used is available in github.com/leoliberti/acopf. Note this is research rather than production code. It is imperfect and may contain bugs.

References

Ahmadi A, Majumdar A (2014) DSOS and SDSOS optimization: LP and SOCP-based alternatives to sum of squares optimization. In: 2014 48th annual conference on information sciences and systems (CISS), pp 1–5

Ahmadi A, Majumdar A (2019) DSOS and SDSOS optimization: more tractable alternatives to sum of squares and semidefinite optimization. SIAM J Appl Algebra Geometry 3(2):193–230

Andersson G (2008) Modelling and Analysis of electric power systems. EEH-Power Systems Laboratory, Swiss Federal Institute of Technology (ETH), Zürich

Anstreicher K (2009) Semidefinite programming versus the reformulation-linearization technique for non-convex quadratically constrained quadratic programming. J Glob Optim 43:471–484

Babaeinejadsarookolaee S, Birchfield A, Christie RD, Coffrin C, DeMarco CL, Diao R, Ferris MC, Fliscounakis S, Greene S, Huang R, Josz C, Korab R, Lesieutre BC, Maeght J, Molzahn DK, Overbye TJ, Panciatici P, Park B, Snodgrass J, Zimmerman R (2019) The power grid library for benchmarking AC optimal power flow algorithms. Technical report. arXiv:1908.02788

Barrows C, Blumsack S, Hines P (2014) Correcting optimal transmission switching for AC power flows. In: 47th Hawaii international conference on system science, pp 2374–2379

Beck A, Beck Y, Levron Y, Shtof A, Tetruashvili L (2018) Globally solving a class of optimal power flow problems in radial networks by tree reduction. J Glob Optim 72:373–402

Bélanger J, Dessaint LA, Kamwa I (2020) An extended optimal transmission switching algorithm adapted for large networks and hydro-electric context. IEEE Access 8:87762–87774

Belotti P, Lee J, Liberti L, Margot F, Wächter A (2009) Branching and bounds tightening techniques for non-convex MINLP. Optim Methods Softw 24(4):597–634

Belotti P, Cafieri S, Lee J, Liberti L (2010) Feasibility-based bounds tightening via fixed points. In: Du D-Z, Pardalos P, Thuraisingham B (eds) Combinatorial optimization, constraints and applications (COCOA10), vol 6508. LNCS. Springer, New York, pp 65–76

Bergen Arthur R, Vijay V (2000) Power systems analysis, 2nd edn. Prentice Hall, Upper Saddle River

Bienstock D (2016) Electrical transmission system cascades and vulnerability: an operations research viewpoint. Number 22 in MOS-SIAM optimization. SIAM, Philadelphia

Bienstock D, Escobar M (2020) Stochastic defense against complex grid attacks. IEEE Trans Control Netw Syst 7(2):842–854
Bienstock D, Muñoz G (2015) Approximate method for AC transmission switching based on a simple relaxation for ACOPF problems. In: 2015 IEEE power and energy society general meeting, pp 1–5
Bienstock D, Verma A (2019) Strong NP-hardness of AC power flows feasibility. Oper Res Lett 47:494–501
Bonnans JF (1997) Mathematical study of very high voltage power networks I: the optimal DC power flow problem. SIAM J Optim 7:979–990
Bonnans JF (1998) Mathematical study of very high voltage power networks II: the AC power flow problem. SIAM J Appl Math 58:1547–1567
Bonnans JF (2000) Mathematical study of very high voltage power networks II: the optimal AC power flow problem. Comput Optim Appl 16:83–101
Bose S, Low S, Teeraratkul T, Hassibi B (2015) Equivalent relaxations of optimal power flow. IEEE Trans Autom Control 60(3):729–742
Brown WE, Moreno-Centeno E (2020) Transmission-line switching for load shed prevention via an accelerated linear programming approximation of ac power flows. IEEE Trans Power Syst 35(4):2575–2585
Cain M, O'Neill R, Castillo A (2012) History of optimal power flow and formulations. Technical Report Staff Paper, Federal Energy Regulatory Commission
Capitanescu F, Wehenkel L (2014) An AC OPF-based heuristic algorithm for optimal transmission switching. In: 2014 power systems computation conference, pp 1–6
Capitanescu F, Glavic M, Ernst D, Wehenkel L (2007) Interior-point based algorithms for the solution of optimal power flow problems. Electric Power Syst Res 77(5):508–517
Carpentier J (1962) Contribution á l'étude du dispatching économique. Bull Société Française des Électriciens 8(3):431–447
Carpentier J (1979) Optimal power flows. Int J Electr Power Energy Syst 1(1):3–15
Chaojun G, Jirutitijaroen P, Motani M (2015) Detecting false data injection attacks in AC state estimation. IEEE Trans Smart Grid 6(5):2476–2483
Coffrin C, Gordon D, Scott P (2014) NESTA. The NICTA energy system test case archive. Technical report. arXiv:1411.0359
Coffrin C, Hijazi H, Van Hentenryck P (2016) The QC relaxation: a theoretical and computational study on optimal power flow. IEEE Trans Power Syst 31(4):3008–3018
Coffrin C, Hijazi H, Van Hentenryck P (2017) Strengthening the SDP relaxation of AC power flows with convex envelopes, bound tightening, and valid inequalities. IEEE Trans Power Syst 32(5):3549–3558
COIN-OR (2006) Introduction to IPOPT: a tutorial for downloading, installing, and using IPOPT
Diamond S, Boyd S (2016) CVXPY: a python-embedded modeling language for convex optimization. J Mach Learn Res 17:1–5
Diestel R (2017) Graph minors. Springer, Berlin, pp 347–391
Domahidi A, Chu E, Boyd S (2013) ECOS: an SOCP solver for embedded systems. In: Proceedings of European control conference, ECC, Piscataway. IEEE
Fisher EB, O'Neill R, Ferris MC (2008) Optimal transmission switching. IEEE Trans Power Syst 23(3):1346–1355
Fourer R, Gay D (2002) The AMPL book. Duxbury Press, Pacific Grove
Frank S, Steponavice I, Rebennack S (2012a) Optimal power flow: a bibliographic survey I. Formulations and deterministic methods. Energy Syst 3:221–258
Frank S, Steponavice I, Rebennack S (2012b) Optimal power flow: a bibliographic survey II. Nondeterministic and hybrid methods. Energy Syst 3:259–289
Ghaddar B, Marecek J, Mevissen M (2016) Optimal power flow as a polynomial optimization problem. IEEE Trans Power Syst 31(1):539–546
Gilbert J-C, Josz C (2017) Plea for a semidefinite optimization solver in complex numbers. Technical Report hal-01422932, HAL Archives-Ouvertes
Gill PE (1999) User's guide for SNOPT 5.3. Systems Optimization Laboratory, Department of EESOR, Stanford University, California
Gleixner AM, Berthold T, Müller B, Weltge S (2017) Three enhancements for optimization-based bound tightening. J Glob Optim 67(4):731–757
Glover JD, Sarma MS, Overbye TJ (2008) Power systems analysis and design, 4th edn. Cengage Learning, Stamford
Gómez Expósito A, Romero Ramos E (1999) Reliable load flow technique for radial distribution networks. IEEE Trans Power Syst 14(3):1063–1069

Gopinath S, Hijazi H, Weißer T, Nagarajan H, Yetkin M, Sundar K, Bent R (2020) Proving global optimality of ACOPF solutions. In: 2020 power systems computation conference, pp 1–6
Hedman KW, O'Neill R, Fisher EB, Oren S (2008) Optimal transmission switching-sensitivity analysis and extensions. IEEE Trans Power Syst 23(3):1469–1479
Henneaux P, Kirschen DS (2016) Probabilistic security analysis of optimal transmission switching. IEEE Trans Power Syst 31(1):508–517
Hijazi H, Coffrin C, Van Hentenryck P (2016) Polynomial SDP cuts for optimal power flow. In: 2016 power systems computation conference, pp 1–7
Hijazi H, Coffrin C, Van Hentenryck P (2017) Convex quadratic relaxations for mixed-integer nonlinear programs in power systems. Math Program Comput 9:321–367
Huneault M, Galiana F (1991) A survey of the optimal power flow literature. IEEE Trans Power Syst 6(2):762–770
Jabr R (2006) Radial distribution load flow using conic programming. IEEE Trans Power Syst 21(3):1458–1459
Jabr R (2007) A conic quadratic format for the load flow equations of meshed networks. IEEE Trans Power Syst 22(4):2285–2286
Jabr R (2008) Optimal power flow using an extended conic quadratic formulation. IEEE Trans Power Syst 23(3):1000–1008
Jabr R (2012) Exploiting sparsity in SDP relaxations of the OPF problem. IEEE Trans Power Syst 27(2):1138–1139
Khanabadi M, Ghasemi H (2011) Transmission congestion management through optimal transmission switching. In: 2011 IEEE power and energy society general meeting, pp 1–5
Khanabadi M, Ghasemi H, Doostizadeh M (2013) Optimal transmission switching considering voltage security and N-1 contingency analysis. IEEE Trans Power Syst 28(1):542–550
Kocuk B, Dey S, Sun XA (2016) Strong SOCP relaxations for the optimal power flow problem. Oper Res 64(6):1177–1196
Kocuk B, Dey S, Sun XA (2017) New formulation and strong MISOCP relaxations for AC optimal transmission switching problem. IEEE Trans Power Syst 32(6):4161–4170
Kocuk B, Dey S, Sun XA (2018) Matrix minor reformulation and SOCP-based spatial branch-and-cut method for the AC optimal power flow problem. Math Program Comput 10(4):557–569
Kuang X, Ghaddar B, Naoum-Sawaya J, Zuluaga L (2016) Alternative LP and SOCP hierarchies for ACOPF problems. IEEE Trans Power Syst 32(4):2828–2836
Lan T, Zhou Z, Huang GM (2018) Modeling and numerical analysis of stochastic optimal transmission switching with DCOPF and ACOPF. IFAC-PapersOnLine 51(28):126–131
Lasserre J (2009) Moments and sums of squares for polynomial optimization and related problems. J Glob Optim 45:39–61
Lavaei J, Low S (2012) Zero duality gap in optimal power flow problem. IEEE Trans Power Syst 27(1):92–107
Lesieutre BC, Molzahn DK, Borden AR, DeMarco CL (2011) Examining the limits of the application of semidefinite programming to power flow problems. In: 2011 49th annual allerton conference on communication, control, and computing (Allerton), pp 1492–1499
Liu X, Li Z (2017) False data attacks against AC state estimation with incomplete network information. IEEE Trans Smart Grid 8(5):2239–2248
Löfberg J (2004) YALMIP: a toolbox for modeling and optimization in MATLAB. In: Proceedings of the international symposium of computer-aided control systems design, volume 1 of CACSD, Piscataway. IEEE
Low S (2013) Convex relaxation of optimal power flow: a tutorial. In: 2013 IREP symposium bulk power system dynamics and control—IX optimization, security and control of the emerging power grid, pp 1–15
Low S (2014a) Convex relaxation of optimal power flow—part I: formulations and equivalence. IEEE Trans Control Netw Syst 1(1):15–27
Low S (2014b) Convex relaxation of optimal power flow—part II: exactness. IEEE Trans Control Netw Syst 1(2):177–189
Lu M, Nagarajan H, Yamangil E, Bent R, Backhaus S, Barnes A (2018) Optimal transmission line switching under geomagnetic disturbances. IEEE Trans Power Syst 33(3):2539–2550
Madani R, Ashraphijuo M, Lavaei J (2016) Promises of conic relaxation for contingency-constrained optimal power flow problem. IEEE Trans Power Syst 31(2):1297–1307

McCormick GP (1976) Computability of global solutions to factorable nonconvex programs: part I—convex underestimating problems. Math Program 10:146–175
Messine F (1997) Méthodes d'optimisation globale basées sur l'analyse d'intervalle pour la résolution de problèmes avec contraintes (in French). Ph.D. thesis, Institut National Polytechnique de Toulouse
Meurer A, Smith C, Paprocki M, Čertík O, Kirpichev S, Rocklin M, Kumar A, Ivanov S, Moore J, Singh S, Rathnayake T, Vig S, Granger B, Muller R, Bonazzi F, Gupta H, Vats S, Johansson F, Pedregosa F, Curry M, Terrel A, Roučka Š, Saboo A, Fernando I, Kulal S, Cimrman R, Scopatz A (2017) SymPy: symbolic computing in Python. PeerJ Comput Sci 3:e103
Molzahn DK, Hiskens IA (2014) Moment-based relaxation of the optimal power flow problem. In: 2014 power systems computation conference, pp 1–7
Molzahn DK, Hiskens IA (2015) Sparsity-exploiting moment-based relaxations of the optimal power flow problem. IEEE Trans Power Syst 30(6):3168–3180
Molzahn DK, Hiskens IA (2019) A survey of relaxations and approximations of the power flow equations. Found Trends® Electric Energy Syst 4(1–2):1–221
Molzahn DK, Holzer JT, Lesieutre BC, DeMarco CL (2013) Implementation of a large-scale optimal power flow solver based on semidefinite programming. IEEE Trans Power Syst 28(4):3987–3998
Molzahn DK, Lesieutre BC, DeMarco CL (2014) A sufficient condition for global optimality of solutions to the optimal power flow problem. IEEE Trans Power Syst 29(2):978–979
Momoh JA, El-Hawary ME, Adapa R (1999a) A review of selected optimal power flow literature to 1993. I. Nonlinear and quadratic programming approaches. IEEE Trans Power Syst 14(1):96–104
Momoh JA, El-Hawary ME, Adapa R (1999b) A review of selected optimal power flow literature to 1993. II. Newton, linear programming and interior point methods. IEEE Trans Power Syst 14(1):105–111
Monticelli A (1999) Power flow equations. Springer, Boston, pp 63–102
Mosek ApS (2016) The `mosek` manual, Version 8
Potluri T, Hedman KW (2012) Impacts of topology control on the ACOPF. In: 2012 IEEE power and energy society general meeting, pp 1–7
Putinar M, Lasserre JB (2011) Positive polynomials and their applications (book review). Found Comput Math 11(4):489–497
Rider MJ, Paucar VL, Garcia AV (2004) Enhanced higher-order interior-point method to minimise active power losses in electric energy systems. IEE Proc Gener Transm Distrib 151(4):517–525
Ruiz M, Maeght J, Marié A, Panciatici P, Renaud A (2014) A progressive method to solve large-scale AC optimal power flow with discrete variables and control of the feasibility. In: Proceedings of the power systems computation conference, volume 18 of PSCC, Piscataway. IEEE
Sahinidis NV, Tawarmalani M (2005) BARON 7.2.5: global optimization of mixed-integer nonlinear programs, user's manual
Salgado E, Gentile C, Liberti L (2018a) Perspective cuts for the ACOPF with generators. In: Daniele P, Scrimali L (eds) New trends in emerging complex real-life problems, volume 1 of AIRO series. Springer, New York, pp 451–461
Salgado E, Scozzari A, Tardella F, Liberti L (2018b) Alternating current optimal power flow with generator selection. In: Lee J, Rinaldi G, Mahjoub R (eds) Combinatorial optimization (proceedings of ISCO 2018), volume 10856 of LNCS, pp 364–375
Shectman JP, Sahinidis NV (1998) A finite algorithm for global minimization of separable concave programs. J Glob Optim 12:1–36
Sherali HD, Alameddine A (1992) A new reformulation-linearization technique for bilinear programming problems. J Glob Optim 2:379–410
Soltan S, Zussman G (July 2017) Power grid state estimation after a cyber-physical attack under the AC power flow model. In: 2017 IEEE power energy society general meeting, pp 1–5
Soroush M, Fuller JD (2014) Accuracies of optimal transmission switching heuristics based on DCOPF and ACOPF. IEEE Trans Power Syst 29(2):924–932
Sridhar S, Hahn A, Govindarasu M (2012) Cyber-physical system security for the electric power grid. Proc IEEE 100(1):210–224
The MathWorks, Inc., Natick, MA (2017) MATLAB R2017a
Tinney WF, Hart CE (1967) Power flow solution by Newton's method. IEEE Trans Power Apparatus Syst PAS–86(11):1449–1460
Torres GL, Quintana VH (1998) An interior-point method for nonlinear optimal power flow using voltage rectangular coordinates. IEEE Trans Power Syst 13(4):1211–1218

Van Ness JE, Griffin JH (1961) Elimination methods for load-flow studies. Trans Am Inst Electr Eng Part III Power Apparatus Syst 80(3):299–302
van Rossum G et al. (2019) Python language reference, version 3. Python Software Foundation
Wang H, Murillo-Sánchez C, Zimmermann R, Thomas R (2007) On computational issues of market-based optimal power flow. IEEE Trans Power Syst 22(3):1185–1193
Wei H, Sasaki H, Kubokawa J, Yokoyama R (1998) An interior point nonlinear programming for optimal power flow problems with a novel data structure. IEEE Trans Power Syst 13(3):870–877
Zamora JM, Grossmann IE (1999) A branch and contract algorithm for problems with concave univariate, bilinear and linear fractional terms. J Glob Optim 14:217–249
Zhao B, Hu Z, Zhou Q, Zhang H, Song Y (2019) Optimal transmission switching to eliminate voltage violations during light-load periods using decomposition approach. J Mod Power Syst Clean Energy 7(2):297–308
Zimmermann R, Murillo-Sánchez C (2018) MatPower 7.0b1 user's manual. Power Systems Engineering Research Center
Zimmermann R, Murillo-Sanchez C, Thomas R (2010) MATPOWER: steady-state operations, planning, and analysis tools for power systems research and education. IEEE Trans Power Syst 26(1):12–19